Baryon dynamics from coupled channels

Michael Doering

Department of Energy,
DOE DE-AC05-06OR23177
& DE-SC0016582

HPC support by JSC
grant *jikp07*

National Science Foundation
Grant No. PHY 2012289

Outline

- Coupled-channel dynamics for the example of $\Lambda(1405)$
- Three-body dynamics: The $a_1(1260)$ and the Roper resonance
- Accessing baryon properties through electroproduction
  - Julich-Bonn-Washington approach

Degrees of freedom: Quarks or hadrons - $\Lambda(1405)$

$\Lambda(1405)$ Review by [Mai 2021]

QCD at low energies

Non-perturbative dynamics → rich spectrum of excited states

How many states are there? → missing resonance problem (does it exist?)

What are they? → 2-quark/3-quark, hadron molecules, …

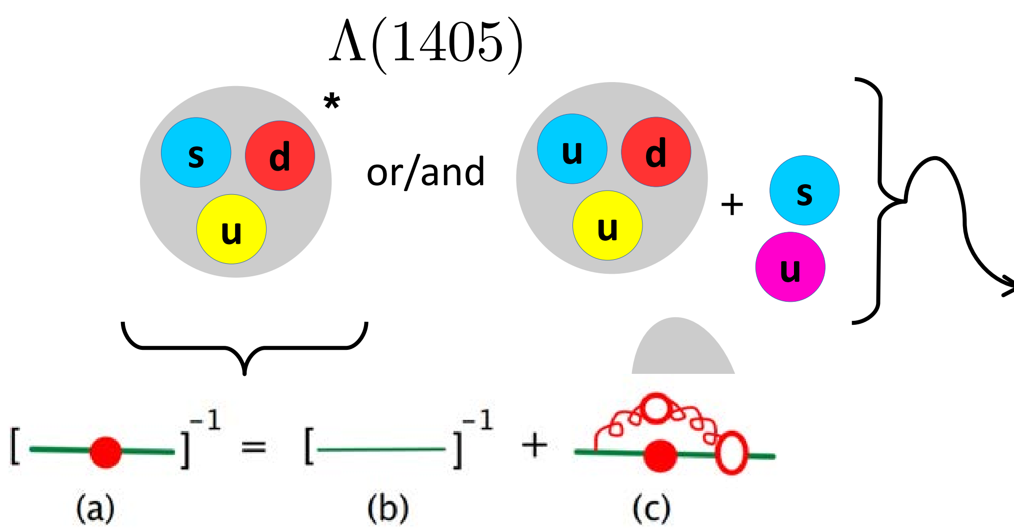

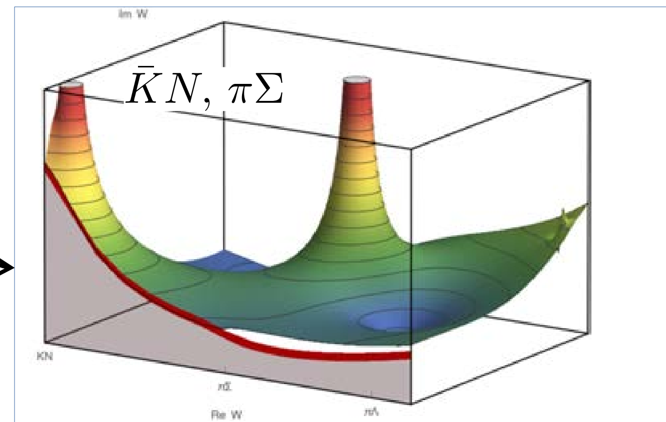

Hadronic molecule

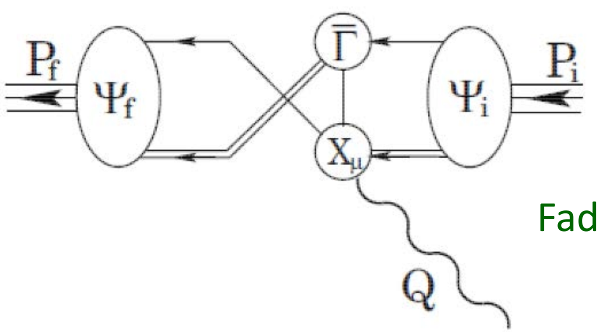

Faddeev Eq. / DSE (Binosi, Cloet, Chang, Eichman, Roberts,…);

Dynamical Diquark picture (DSE)

Quark-diquark with reduced pseudoscalar + vector diquarks: [Eichmann (2016)]

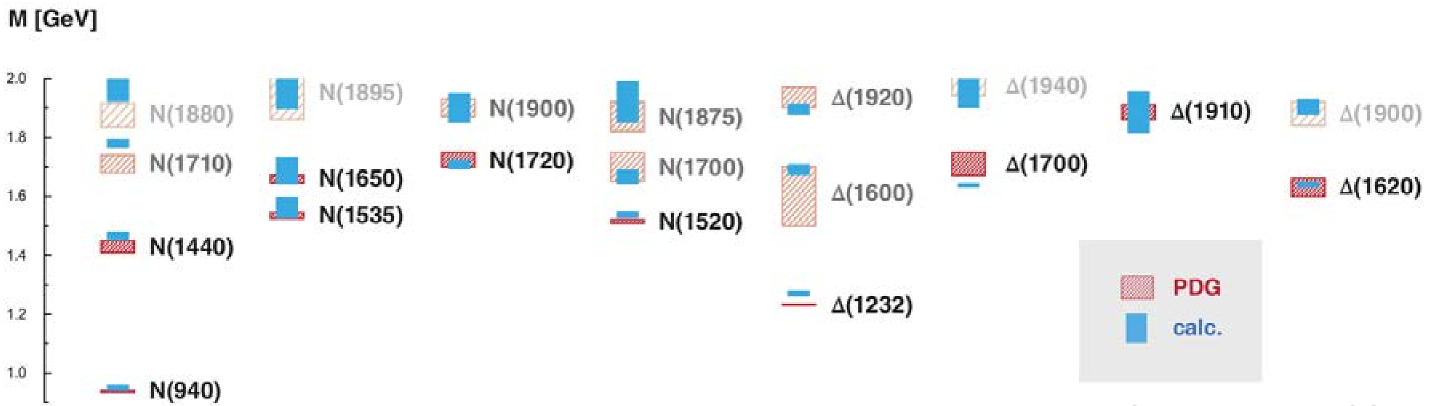

[parts of slide courtesy of G. Eichmann, Few Body 2018]

$J^P = \frac{1}{2}^+ \quad \frac{1}{2}^- \quad \frac{3}{2}^+ \quad \frac{3}{2}^- \quad \frac{3}{2}^+ \quad \frac{3}{2}^- \quad \frac{1}{2}^+ \quad \frac{1}{2}^-$

Poincaré-covariant analysis of heavy-quark baryons, [Qin 2018]
Spectrum of light- and heavy-baryons, [Qin 2019]

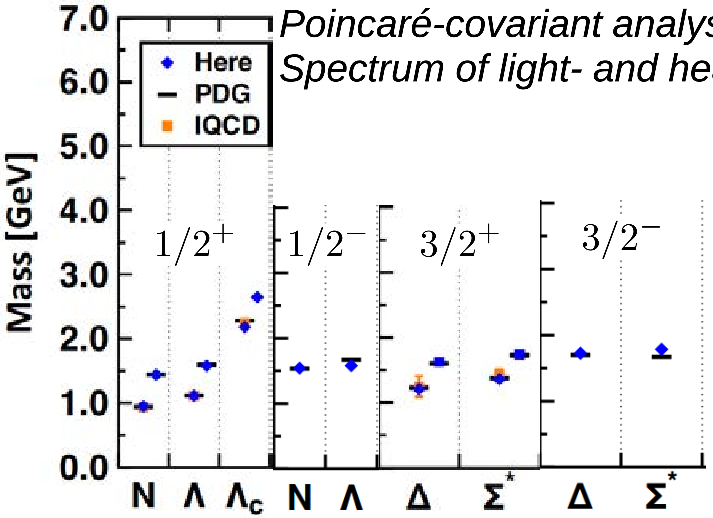

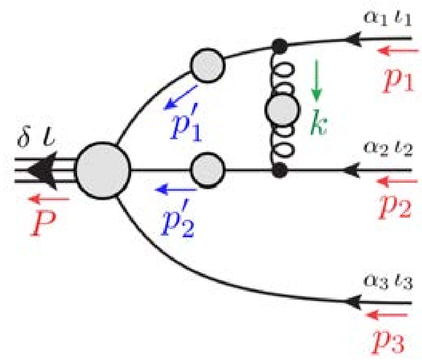

Decades-long interest in S=-1 low energy

- From Dalitz [PRL 1959] to NNLO treatment connecting all strangeness sectors [J.-Xu Lu (2022)]
- Main question: How does chiral dynamics dictate the low-energy, coupled-channel $\bar{K}N$ interaction?
  - Inherently non-perturbative
  - Expansion of chiral kernels to different chiral orders with subsequent unitarization
- Ten channels in isospin-0 and I=1, usually with mass differences

$$\pi^0\Lambda,\ \pi^-\Sigma^+,\ \pi^0\Sigma^0,\ \pi^+\Sigma^-,\ K^-p,\ \bar{K}^0n,\ \eta\Lambda,\ \eta\Sigma^0,\ K^0\Xi^0,\ K^+\Xi^-$$

- Their interaction to
  - LO [Kaiser (1995), Oset (1998), Oller (2001), Jido (2003); ~700 citations each],
  - NLO [Mai (2014), Z. H. Guo (2012)],
  - NNLO [J.-Xu Lu (2022)]
- Full Bethe-Salpeter equation in [Mai (2014)]

$$T(\not{q}_2,\not{q}_1;p) = V(\not{q}_2,\not{q}_1;p) + i\int \frac{d^d\ell}{(2\pi)^d}\frac{V(\not{q}_2,\not{\ell};p)}{\ell^2 - M^2 + i\epsilon}\frac{1}{\not{p}-\not{\ell}-m+i\epsilon}T(\not{\ell},\not{q}_1;p), \qquad (1)$$

Interconnecting meson-baryon strangeness sectors at NNLO [J.-Xu Lu, L.S. Geng, MD, Mai 2022]

- First simultaneous study of meson-baryon interaction of
  - Strangeness S=0: (πN) Perturbative [SAID WI08 phases]
  - S=+1 (KN) Perturbative [SAID SP92]
  - S=-1: $(\bar{K}N$ in 10 chann.) Unitarized exp. data
- Chiral convergence poor for S=0:
  - One really needs NNLO for a global analysis
  - extended-on-mass-shell (EOMS) formulation of BCHPT improves convergence in $SU(3)_f$
- NNLO has more parameters (33) than NLO (20),
  - but interconnection of data sectors (for 1^{st} time) leads to **smaller** uncertainties than NLO due to much larger, "orthogonal" data base.

Results – Data description in S=-1

[J.-Xu Lu 2022]

- Strangeness sector:
  - $x^2/dof = 1.56$ at NNLO with constraints from strangeness S=0 and S=+1
  - compare: x^2/dof =2 at NLO [Z. H. Guo (2012)] without add. constraints

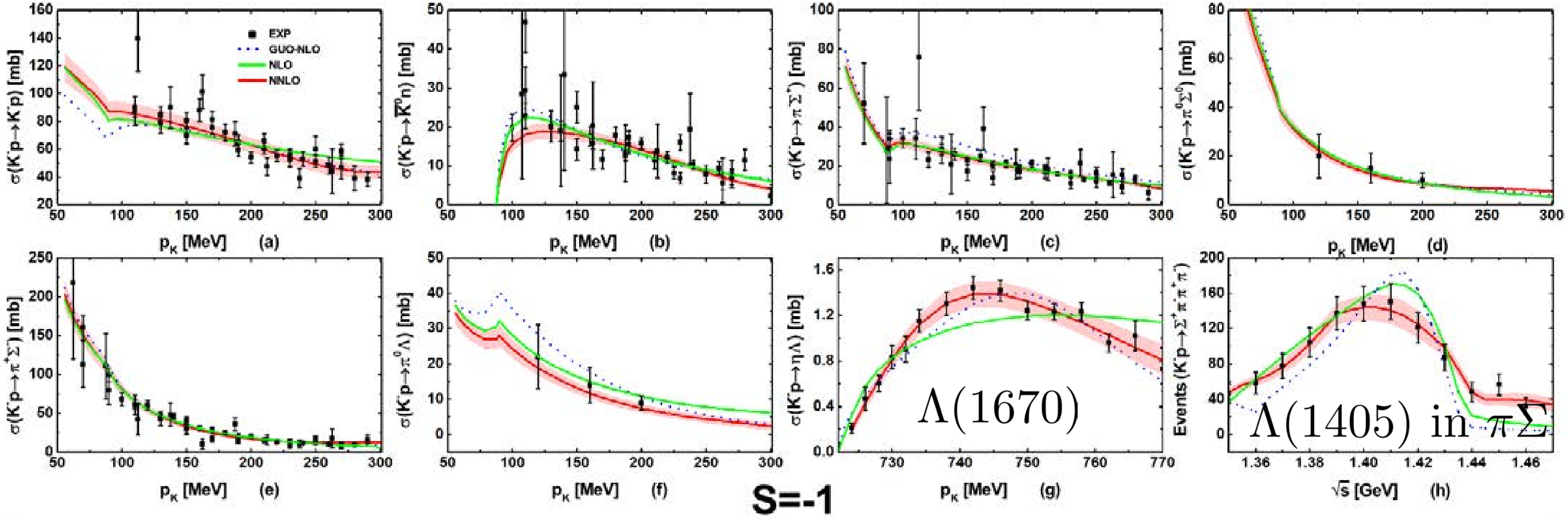

(and threshold quantities/not shown)

Results – PW description in S=0, +1

[J.-Xu Lu 2022]

- Compare NLO and NNLO
  - NNLO needed!
- Uncertainty bands from truncation of chiral expansion (dominant error)

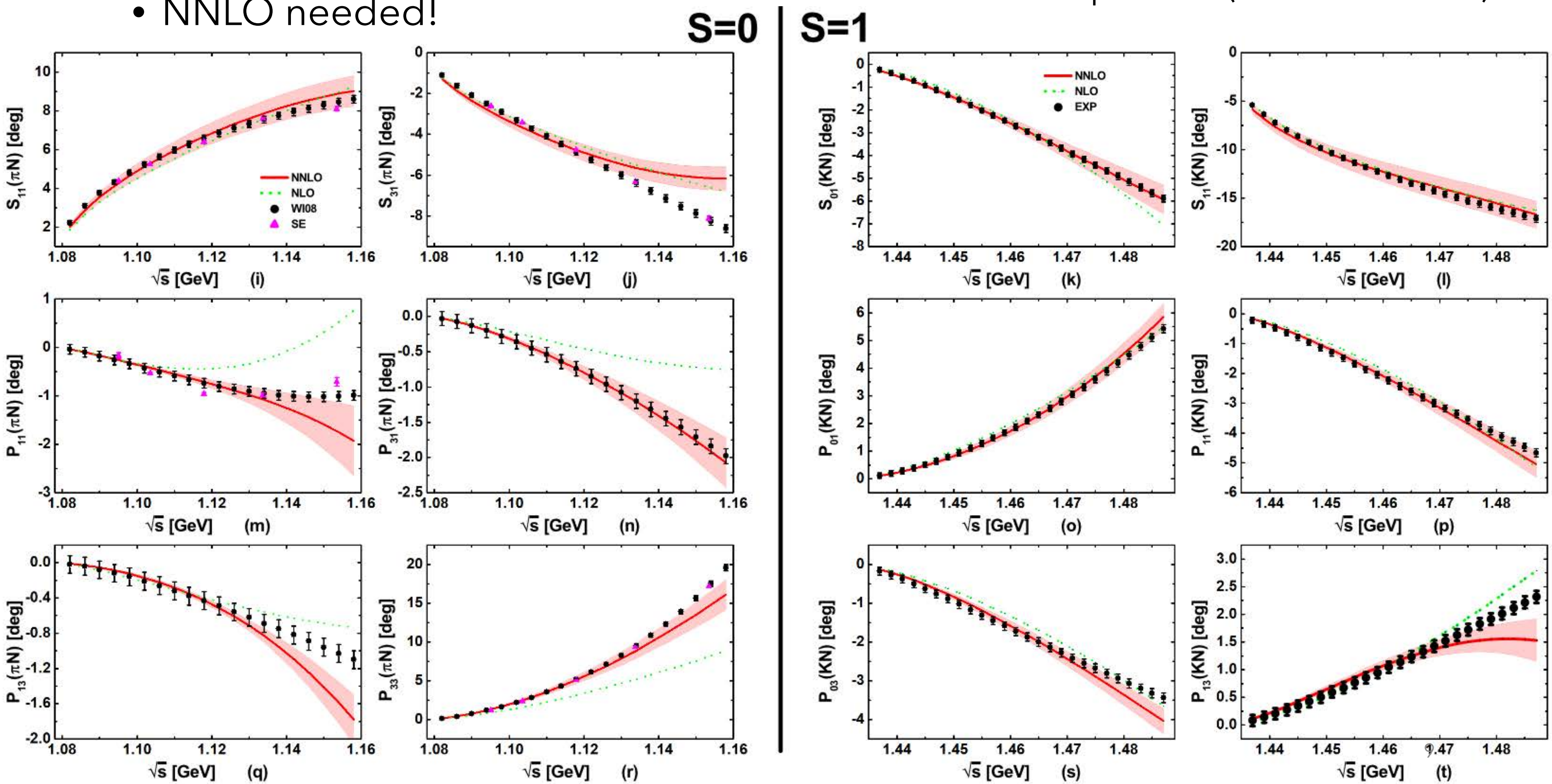

Two-pole structure of $\Lambda(1405)$ confirmed

[J.-Xu Lu 2022]

- with smaller uncertainties than at NLO, due to global data analysis.

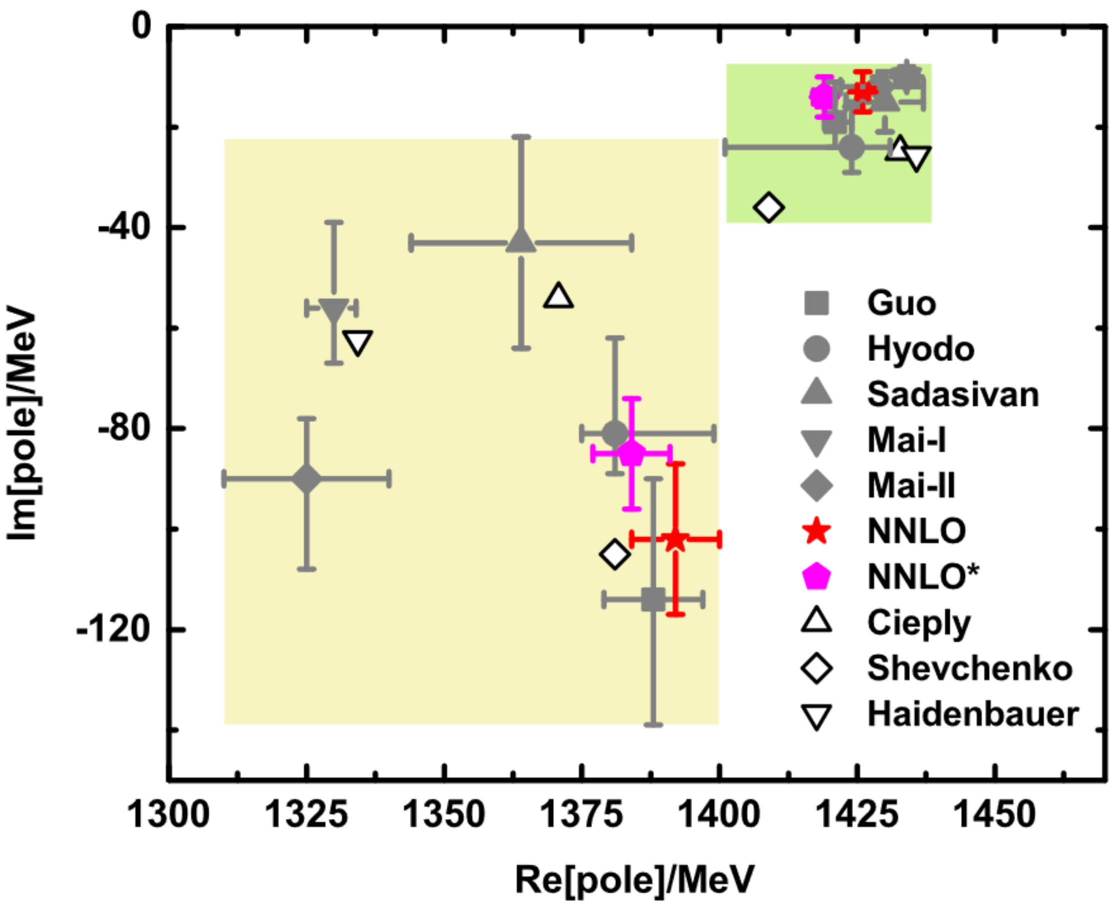

- **NNLO**: Main result
- **NNLO***: Fit without constraints from baryon masses

Lattice QCD for excited baryons/ 3-body systems

Review: resonances from lQCD [Mai, Meißner, Urbach 2022]
Review: 2B-resonances lattice: [Briceno 2017]
Reviews 3B-lattice: [Hansen 2019] [Mai 2021]

Lattice QCD for excited baryons

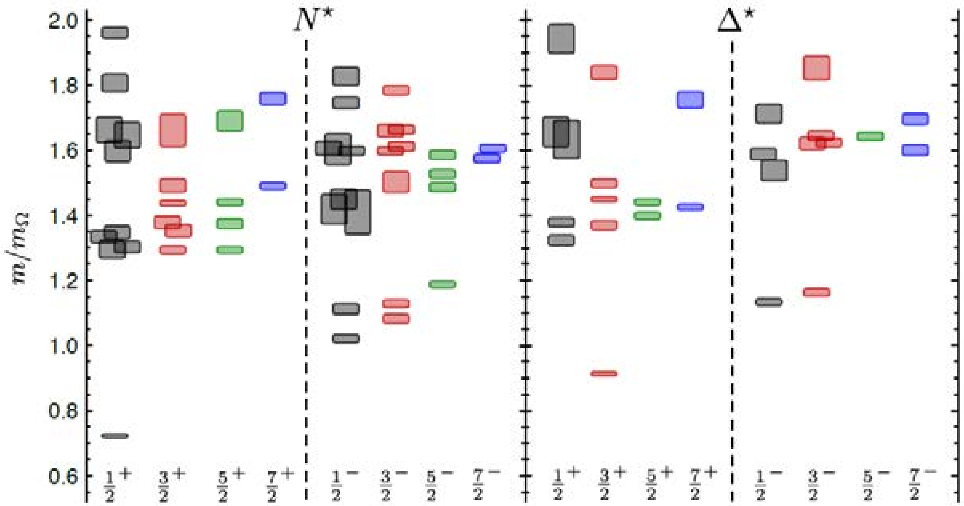

$m_\pi = 396$ MeV [Edwards *et al.*, Phys.Rev. D84 (2011)]

- Pioneering spectroscopic calculations
- Information on existence, width & properties of resonances requires
  - Meson-baryon interpolating operators
  - Detailed finite-volume analysis

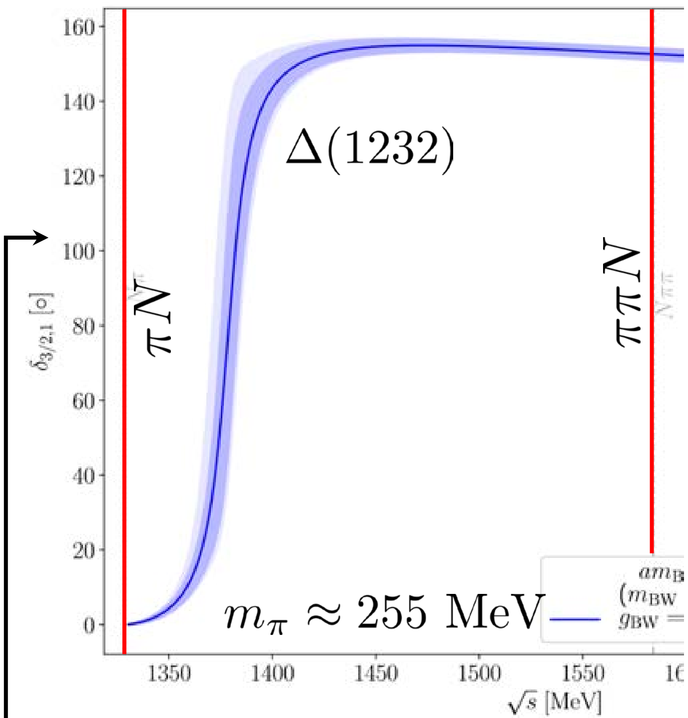

[G. Silvi et. al., arXiv: 2101.00689]
See also: Bulava et al., [2208.03867]

How about $\pi\pi N$? Roper resonance?

Three-body aspects: $\pi\pi N$ vs. $\pi\pi\pi$

Light mesons

- COMPASS @ CERN: $\pi_1(1600)$ discovery
- GlueX @ Jlab in search of hybrids and exotics,
- Finite volume spectrum from lattice QCD:
  Lang (2014), Woss [HadronSpectrum] (2018) Hörz (2019), Culver (2020), Fischer (2020), Hansen (2020),...

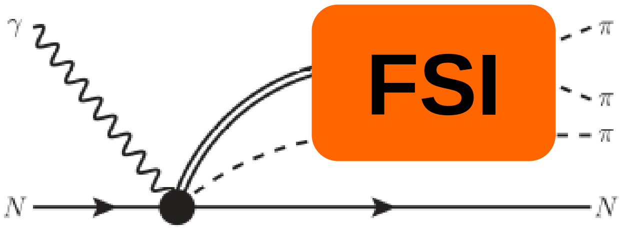

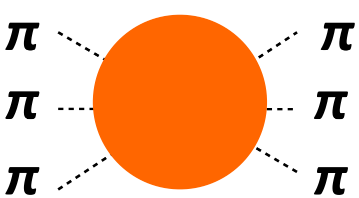

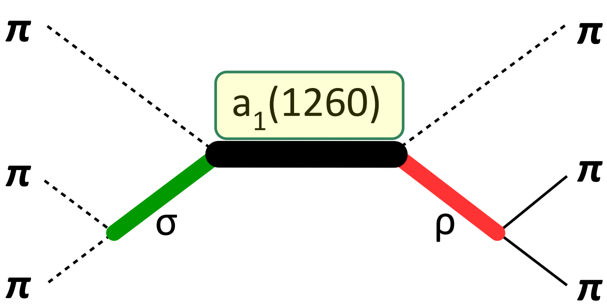

Light baryons

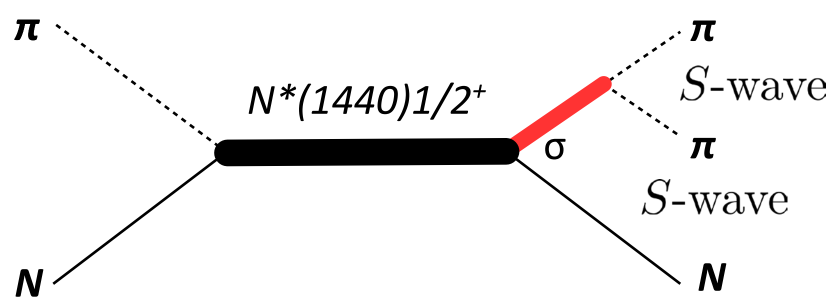

- Roper resonance is debated for ~50 years in experiment. Can only be seen in PWA.
- 1st calculation w. meson-baryon operators on the lattice: **Lang et al. (2017)**

Lattice QCD for three-body resonances

- First-ever three-body resonance from 1st principles (with explicit three-body dynamics). [Mai/GWQCD, PRL 2021]

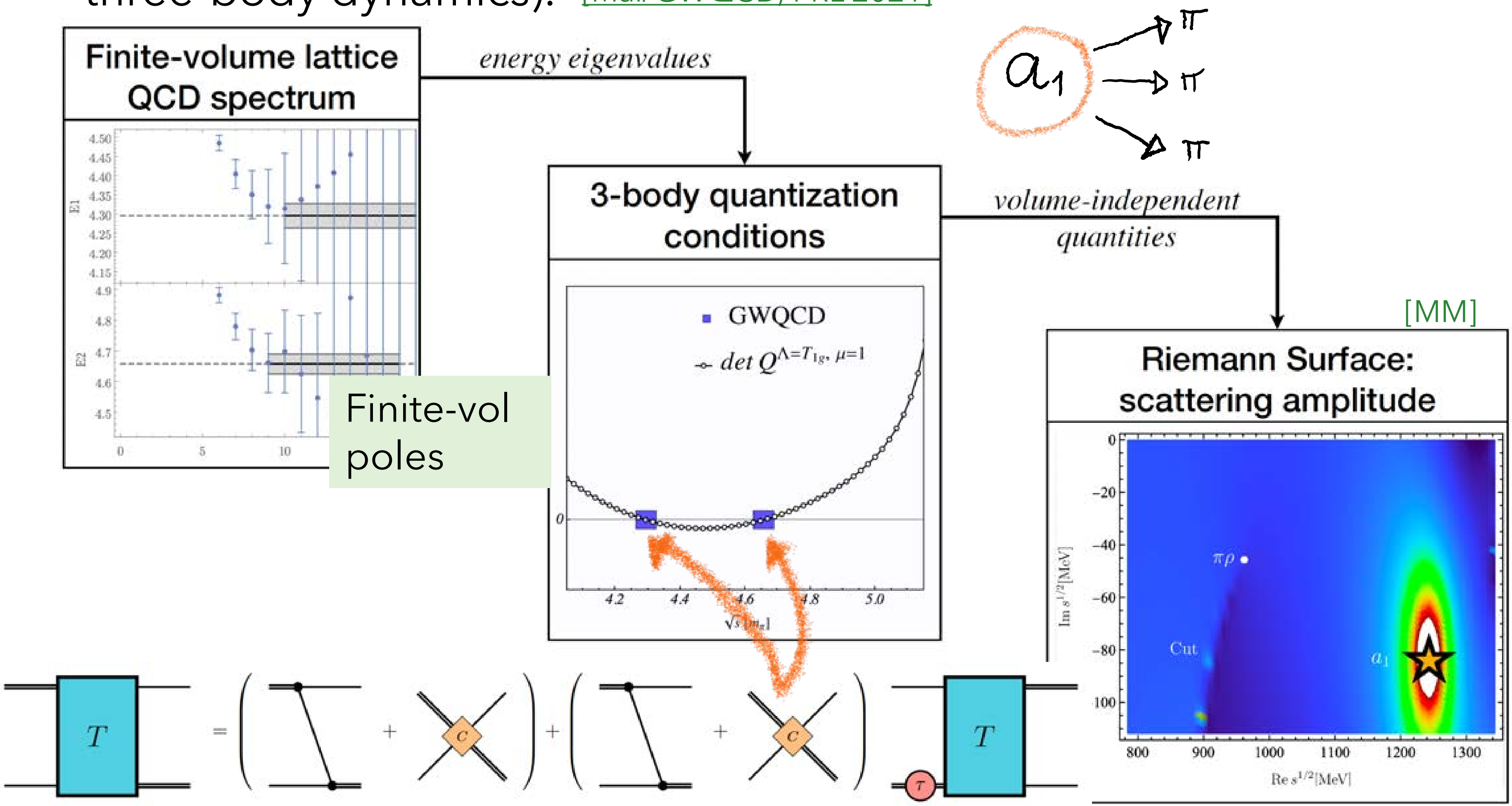

Extraction of $a_1(1260)$ from lQCD [Mai/GWQCD, PRL 2021]

$\tau \to (\pi\pi\pi)\nu_\tau$

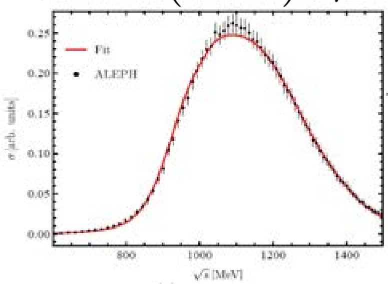

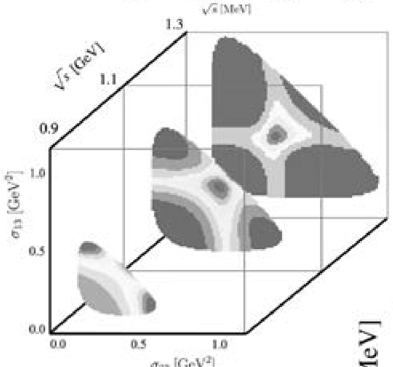

[Sadasivan 2020]
[Sadasivan 2022]

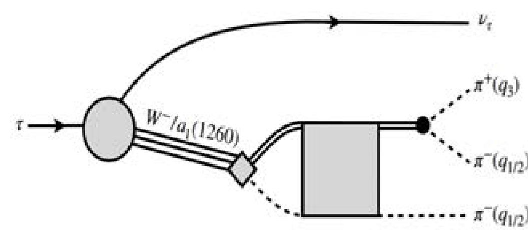

- Two mass-degenerate light quarks (u,d); valence strange quark
- nHYP-smeared clover action
- quark propagation is treated using the LapH method with optimized inverters
- Lattice spacing determined from Wilson flow parameter w_0

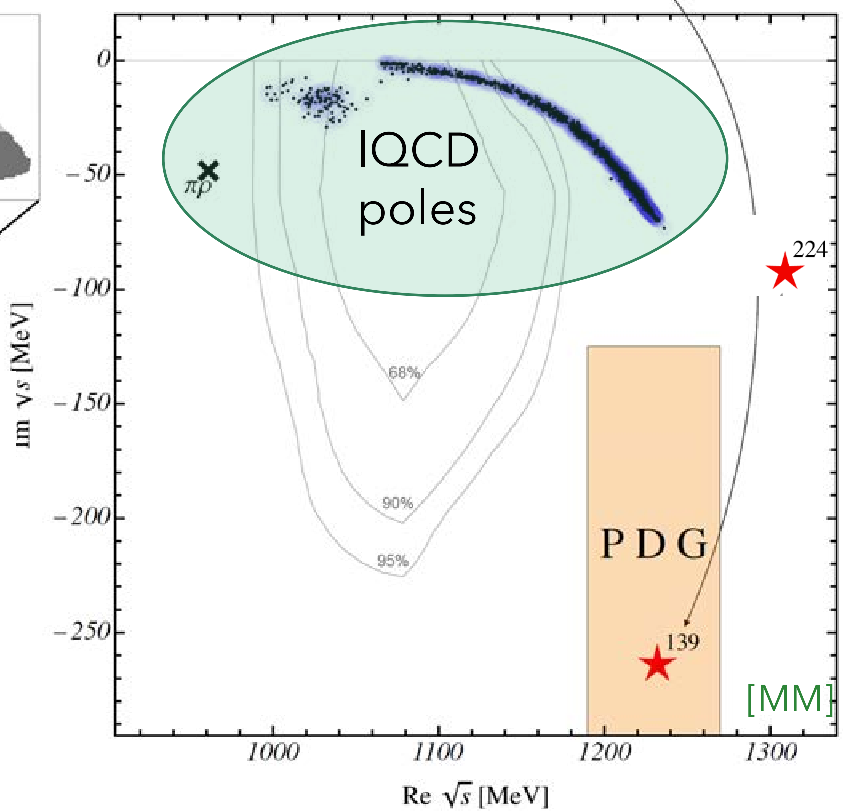

"**Branching ratios**" in 3B decays are momentum – dependent, complex pole residues

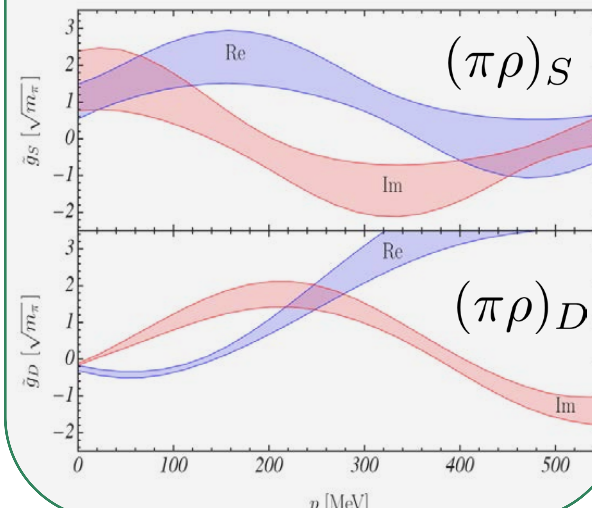

Three-body effects in the Roper Resonance: Challenge for lQCD

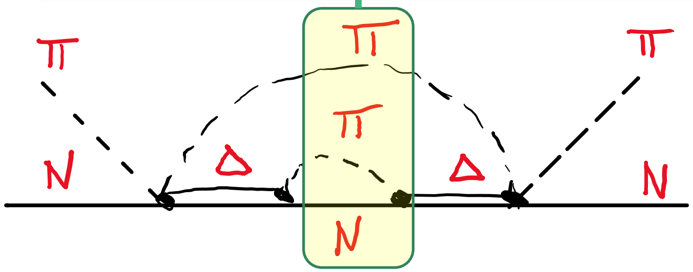

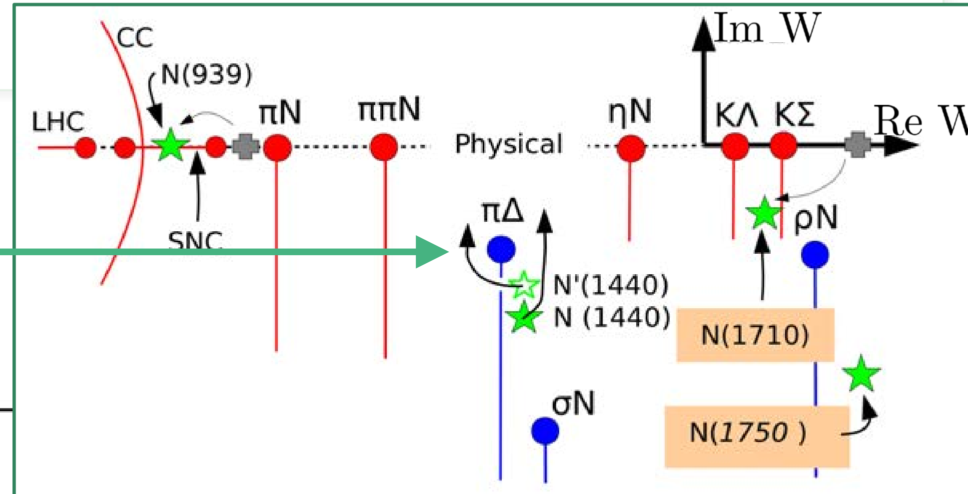

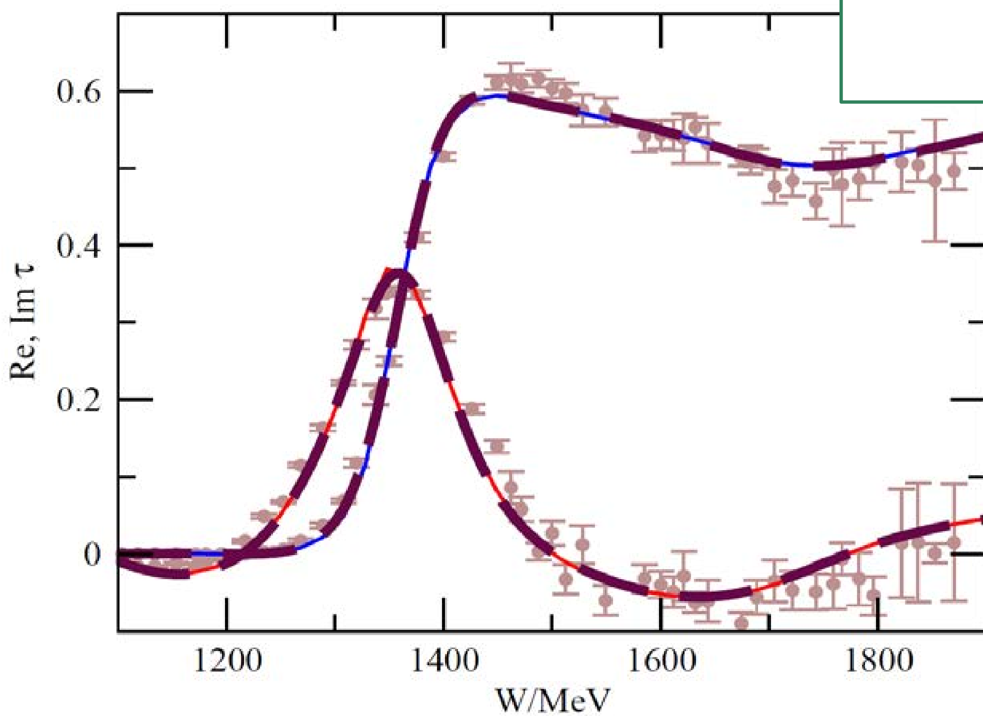

Strategy for data analysis:

- manifestly include all known analytic structures into the model amplitude before fitting to data
- Respect unitarity, analyticity,…

Phenomenology of the baryon spectrum

Review by [Thiel, Afzal, Wunderlich 2022]

Dynamical coupled-channel approaches

- ANL-Osaka (former: EBAC) [Kamano et al.]
- Dubna-Mainz-Taipei model [Tiator]
- Jülich-Bonn(-Washington) [Rönchen]
- …
- Characteristics:
  - Direct fit to data (pion & photon-induced)
  - Simultaneous fit to data of different final states
  - Integral scattering equation as needed for proper treatment of three-body channels ($\pi\pi N$)

Note: Only a sub-class of analysis efforts; see, e.g., Bonn-Gatchina group K-matrix approach

JBW DCC approach (Jülich-Bonn-Washington)

The scattering equation in partial-wave basis

$$\langle L'S'p'|T^{IJ}_{\mu\nu}|LSp\rangle = \langle L'S'p'|V^{IJ}_{\mu\nu}|LSp\rangle + \sum_{\gamma,L''S''}\int_0^\infty dq\; q^2\; \langle L'S'p'|V^{IJ}_{\mu\gamma}|L''S''q\rangle \frac{1}{E-E_\gamma(q)+i\epsilon} \langle L''S''q|T^{IJ}_{\gamma\nu}|LSp\rangle$$

- channels ν, μ, γ:

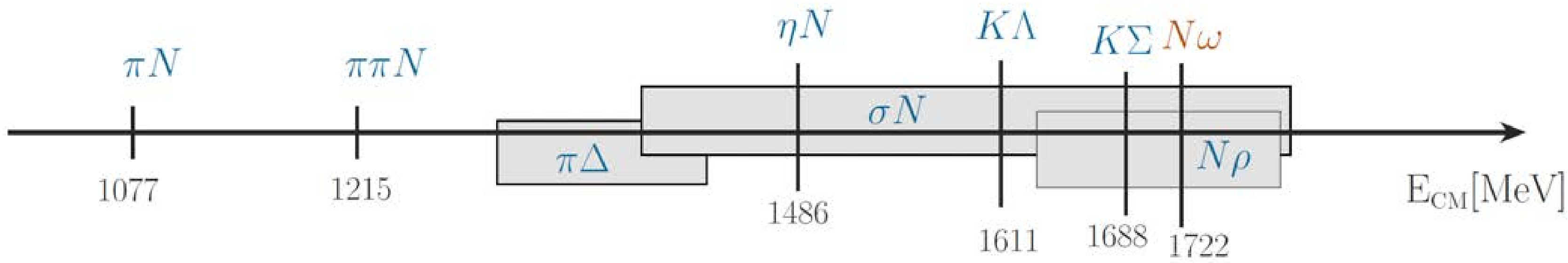

JBW DCC approach (Jülich-Bonn-Washington)

The scattering equation in partial-wave basis

$$\langle L'S'p'|T^{IJ}_{\mu\nu}|LSp\rangle = \langle L'S'p'|V^{IJ}_{\mu\nu}|LSp\rangle + \sum_{\gamma,L''S''}\int_0^\infty dq\; q^2\; \langle L'S'p'|V^{IJ}_{\mu\gamma}|L''S''q\rangle \frac{1}{E-E_\gamma(q)+i\epsilon}\langle L''S''q|T^{IJ}_{\gamma\nu}|LSp\rangle$$

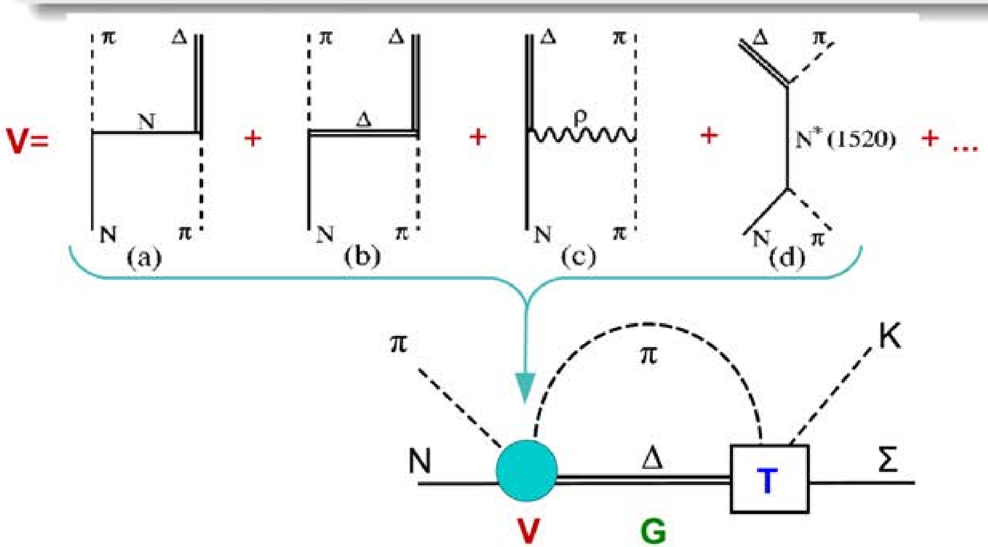

- potentials V constructed from effective $\mathcal{L}$
- s-channel diagrams: T^P
  genuine resonance states
- t- and u-channel: T^{NP}
  dynamical generation of poles
  partial waves strongly correlated
- contact terms

Three-body channels $\sigma N, \pi\Delta, \rho N$

- Resonant sub-channels
- Fit 2→2 amplitude to 2→ 2 scattering data
- Include as sub-channel in 3-body amplitude:
- 3-body unitarity: Requires, e.g.

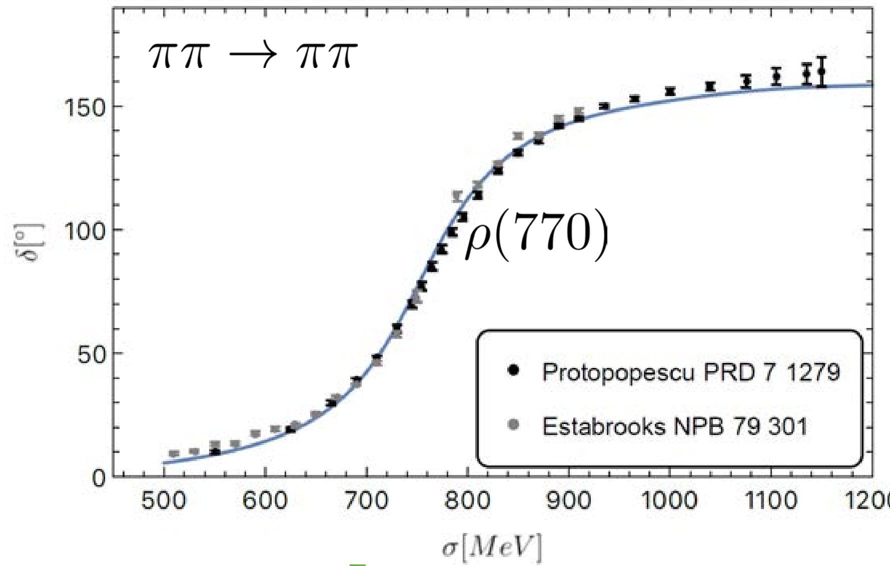

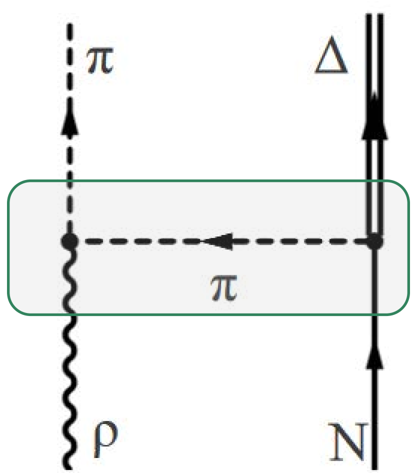

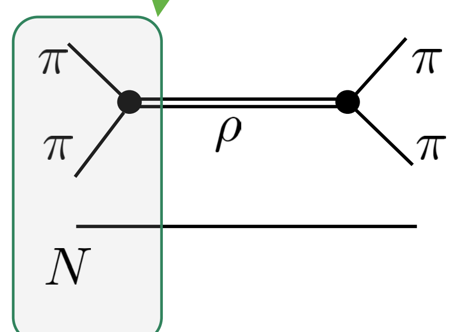

JBW: Photoproduction Data base

- $\pi N \to X$: $>$ **7,000** data points ($\pi N \to \pi N$: GW-SAID WI08 (ED solution))
- $\gamma N \to X$:

New: $\pi N \to \omega N$ [2208.03061]
Upcoming data from JParc

Reaction	Observables (# data points)	p./channel
$\gamma p \to \pi^0 p$	$d\sigma/d\Omega$ (18721), Σ (2927), P (768), T (1404), $\Delta\sigma_{31}$ (140),	
	G (393), H (225), E (467), F (397), $C_{x'_L}$ (74), $C_{z'_L}$ (26)	25,542
$\gamma p \to \pi^+ n$	$d\sigma/d\Omega$ (5961), Σ (1456), P (265), T (718), $\Delta\sigma_{31}$ (231),	
	G (86), H (128), E (903)	9,748
$\gamma p \to \eta p$	$d\sigma/d\Omega$ (9112), Σ (403), P (7), T (144), F (144), E (129)	9,939
$\gamma p \to K^+\Lambda$	$d\sigma/d\Omega$ (2478), P (1612), Σ (459), T (383),	
	$C_{x'}$ (121), $C_{z'}$ (123), $O_{x'}$ (66), $O_{z'}$ (66), O_x (314), O_z (314),	5,936
$\gamma p \to K^+\Sigma^0$	$d\sigma/d\Omega$ (4271), P (422), Σ (280), T (127), $C_{x',z'}$ (188), $O_{x,z}$ (254)	5,542
$\gamma p \to K^0\Sigma^+$	$d\sigma/d\Omega$ (242), P (78)	320
	in total	**57,027**

A new web interface [https://jbw.phys.gwu.edu/]

Resonances in $K\Sigma$ photoproduction

- [D. Roenchen et al., 2208.00089]
- [Webpage all results]

$\gamma p \to K^+\Sigma^0$

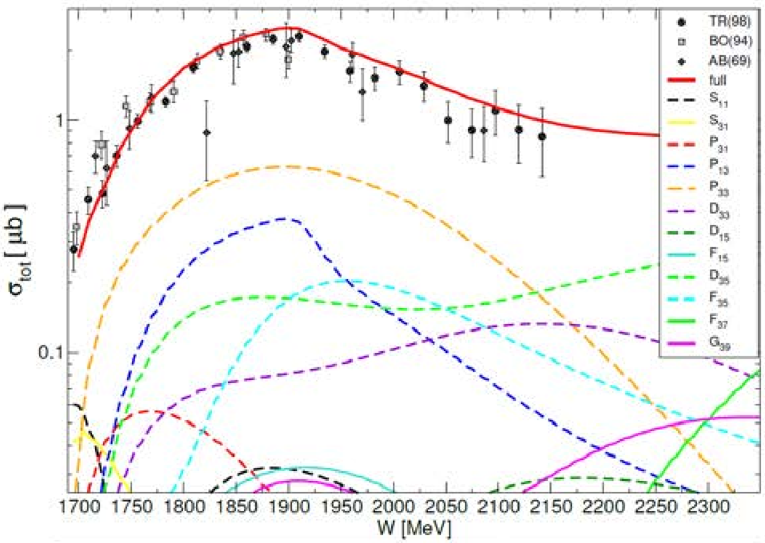

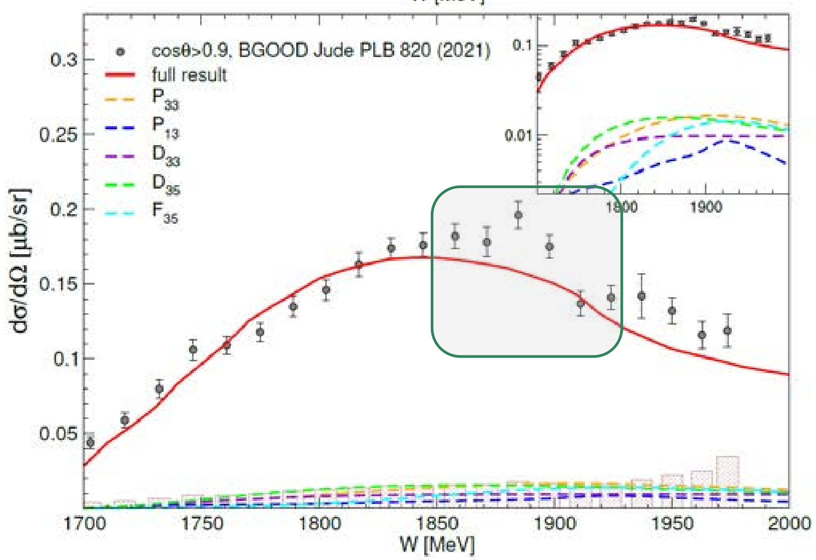

- dominant partial waves: $I = 3/2$

Exception: P_{13} partial wave ($I = 1/2$):

$N(1720)\ 3/2^+$ ∗ ∗ ∗∗	Re E_0 [MeV]	$-2\text{Im}\ E_0$ [MeV]	$\frac{\Gamma^{1/2}_{\pi N}\Gamma^{1/2}_{K\Sigma}}{\Gamma_{tot}}$ [%]	$\theta_{\pi N\to K\Sigma}$ [deg]
2022	1726	185	5.9	82
2017	1689(4)	191(3)	0.6(0.4)	26(58)
PDG 2021	1675 ± 15	250^{+150}_{-100}	—	—

$N(1900)\ 3/2^+$ ∗ ∗ ∗∗	Re E_0 [MeV]	$-2\text{Im}\ E_0$ [MeV]	$\frac{\Gamma^{1/2}_{\pi N}\Gamma^{1/2}_{K\Sigma}}{\Gamma_{tot}}$ [%]	$\theta_{\pi N\to K\Sigma}$ [deg]
2022	1905	93	1.3	−40
2017	1923(2)	217(23)	10(7)	−34(74)
PDG 2021	1920±20	150±50	4±2	110±30

- drop in cross section ("cusp-like structure") due to $N(1900)3/2^+$

$N(1535)$ ½⁻ ∗ ∗ ∗∗	Re E_0 [MeV]	$-2\text{Im}\ E_0$ [MeV]
2022	1504(0)	74 (1)
2017	1495(2)	112(1)
PDG 2021	1510 ± 10	130 ± 20

Compare V. Crede's talk Baryons 2022

Pion and eta Electroproduction

First coupled-channel electroproduction analysis with different final states

[M. Mai et al., 2104.07312 [nucl-th], 2111.04774 (PRC)]

Electroproduction reveals resonance structure

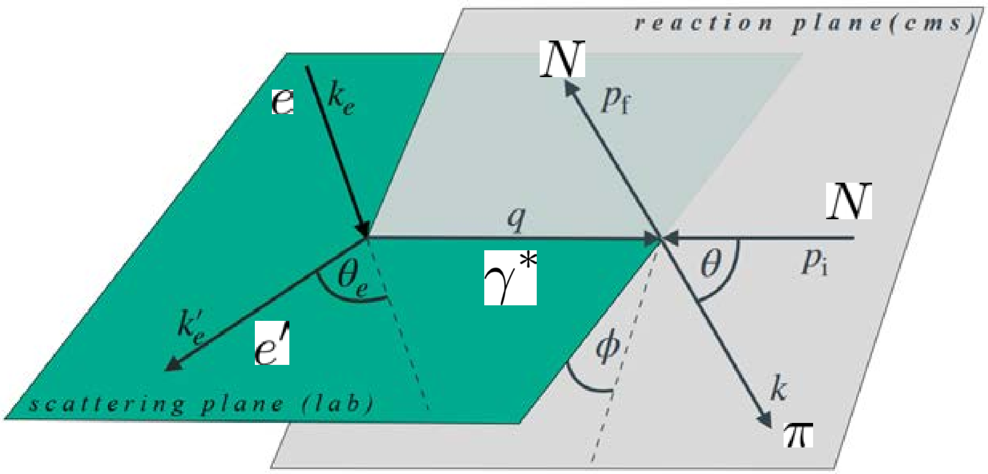

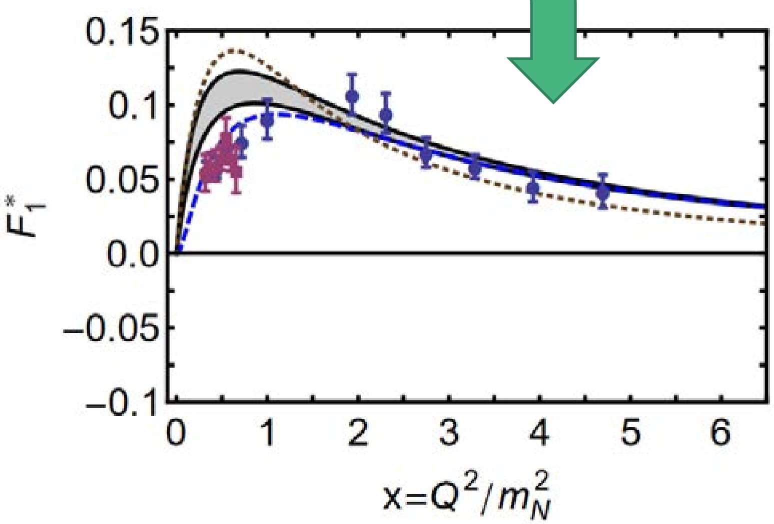

Proton-Roper Transition [Burkert] [Segovia]

Photoproduction included as boundary

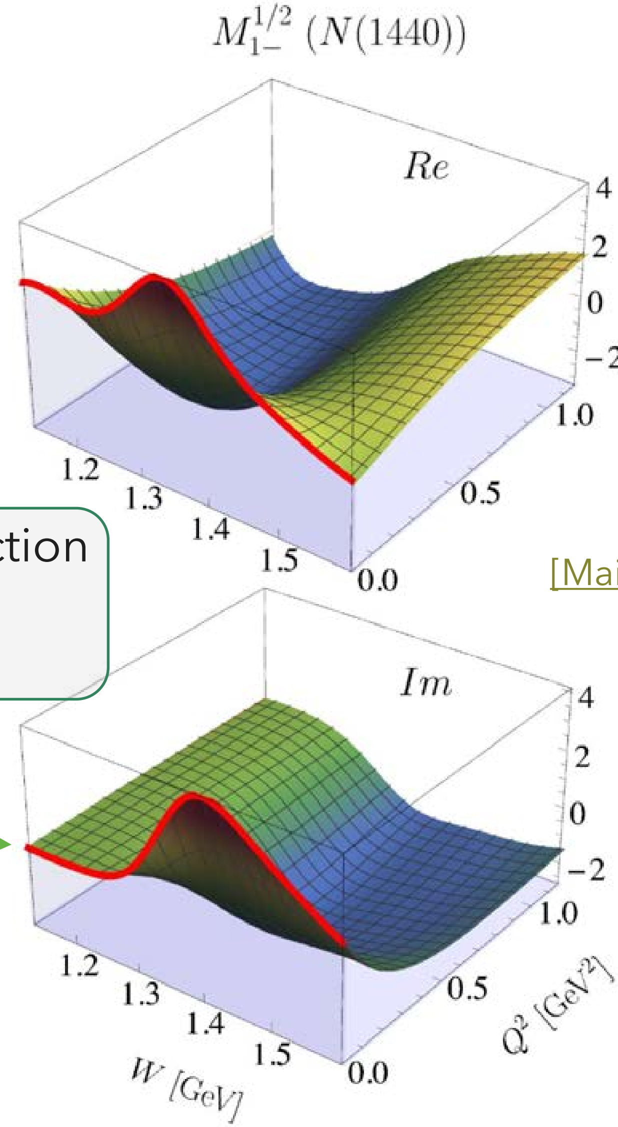

[Mai]

Fit Strategies

- Different fit strategies for $N \approx 85{,}000$ data in $\gamma^* N \to \pi N, \eta N$:
  - Sequential S → S+P → S+P+D waves;
  - Subsets of data until full data set reached
  - Simultaneous fit all parameters (209) set to zero without any (!) guidance
  - Extend data range from $0 < Q^2 < 4$ Gev² to $0 < Q^2 < 6$ Gev² to check for stability

Fit	σ_L		$d\sigma/d\Omega$		$\sigma_T + \epsilon\sigma_L$		σ_T		σ_{LT}		$\sigma_{LT'}$		σ_{TT}		K_{D1}		P_Y		ρ_{LT}		$\rho_{LT'}$		$\chi^2_{\rm dof}$
	$\pi^0 p$	$\pi^+ n$	$\pi^0 p$	$\pi^+ n$	$\pi^0 p$	$\pi^+ n$	$\pi^0 p$	$\pi^+ n$	$\pi^0 p$	$\pi^+ n$	$\pi^0 p$	$\pi^+ n$	$\pi^0 p$	$\pi^+ n$	$\pi^0 p$	$\pi^+ n$	$\pi^0 p$	$\pi^+ n$	$\pi^0 p$	$\pi^+ n$	$\pi^0 p$	$\pi^+ n$	
$\mathfrak{F}_1$	–	9	65355	53229	870	418	87	88	1212	133	862	762	4400	251	4493	–	234	–	525	–	3300	10294	1.77
$\mathfrak{F}_2$	–	4	69472	55889	1081	619	65	78	1780	150	1225	822	4274	237	4518	–	325	–	590	–	3545	10629	1.69
$\mathfrak{F}_3$	–	8	66981	54979	568	388	84	95	1863	181	1201	437	3934	339	4296	–	686	–	687	–	3556	9377	1.81
$\mathfrak{F}_4$	–	22	63113	52616	562	378	153	107	1270	146	1198	1015	4385	218	5929	–	699	–	604	–	3548	11028	1.78
$\mathfrak{F}_5$	–	20	65724	53340	536	528	125	81	1507	219	1075	756	4134	230	5236	–	692	–	554	–	3580	11254	1.81
$\mathfrak{F}_6$	–	18	71982	58434	1075	501	29	68	1353	135	1600	1810	3935	291	5364	–	421	–	587	–	3932	11475	1.78

χ^2

Description of Polarization Observables

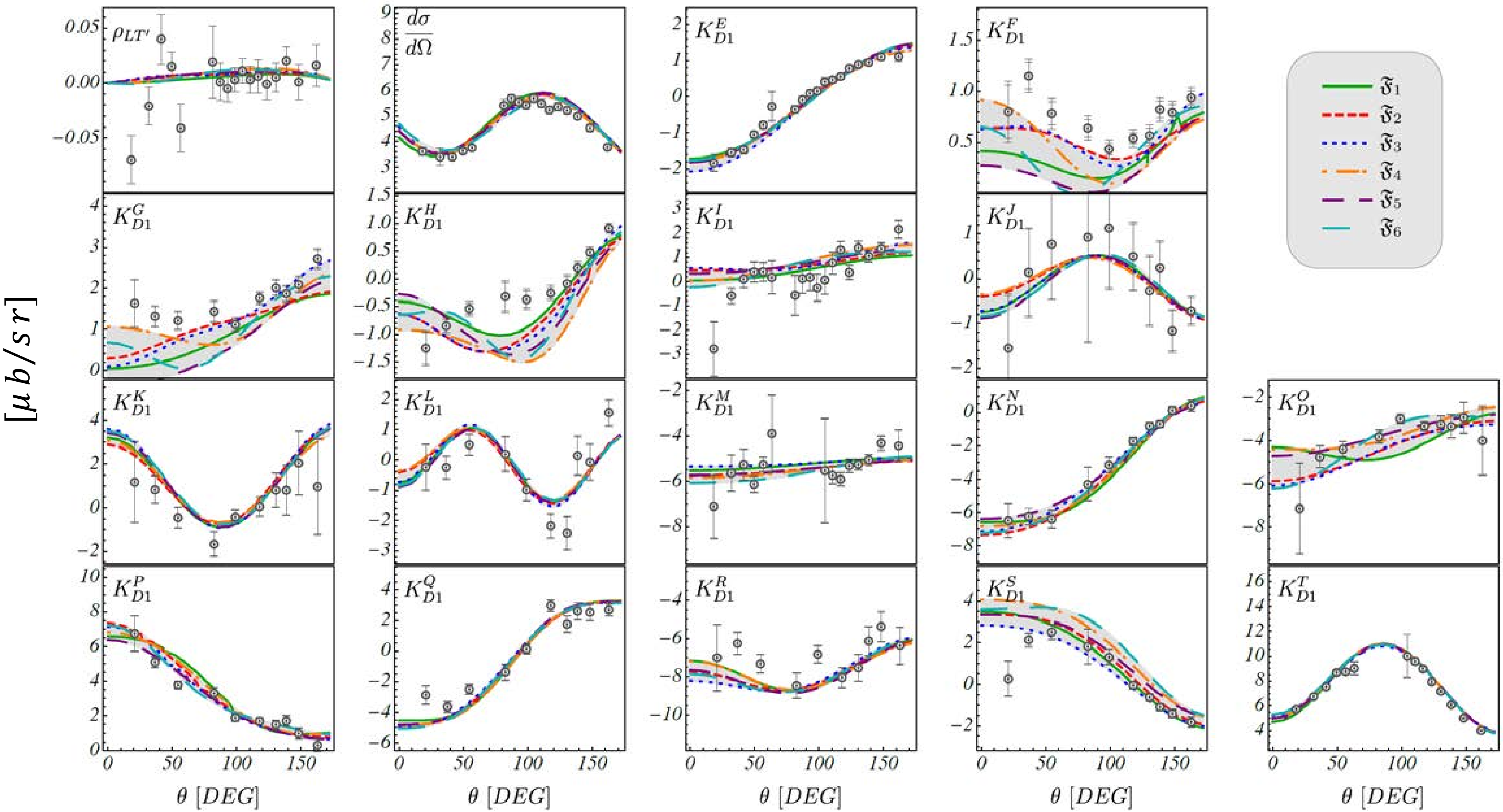

$\pi^0 p$, $Q^2=1$ GeV^2, W=1.23 GeV, $\phi=15^0$

J. J. Kelly, Phys. Rev. Lett. 95 (2005).

Large Multipoles

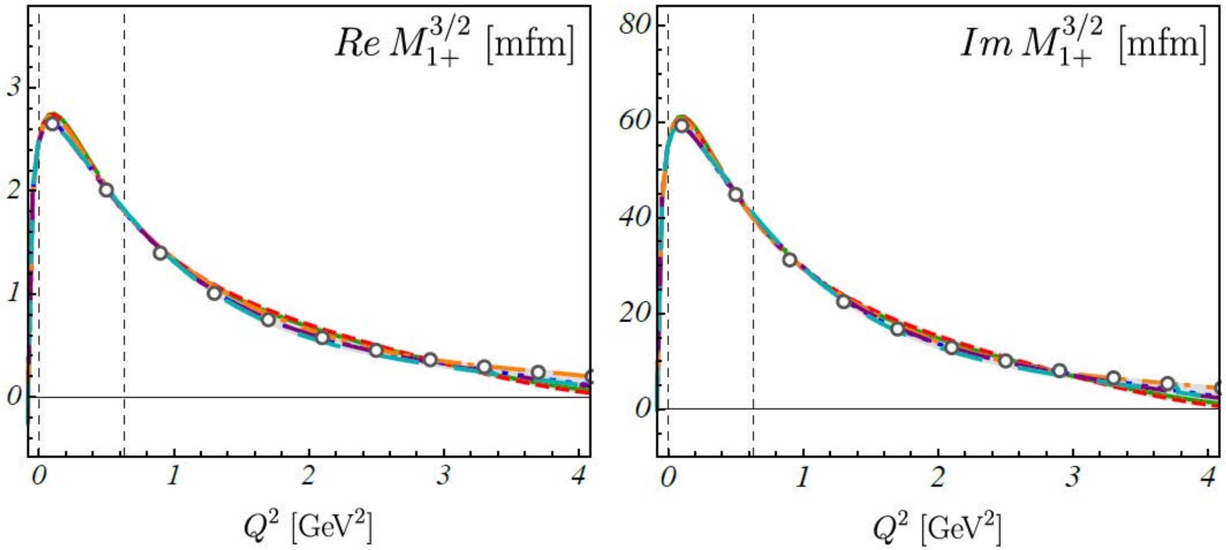

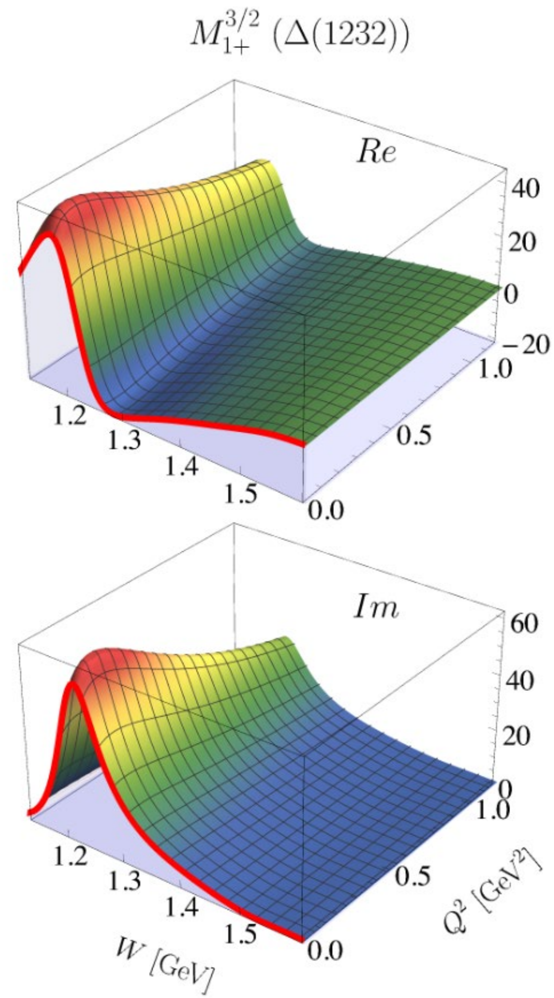

Fit strategies 1-6 together with MAID (open dots) for the magnetic multipole of the $\Delta(1232)$ Drechsel et al., EPJA (2007) 0710.0306 [nucl-th]

Prominent multipoles are well determined

(Strategy 1 only)

Roper Multipole

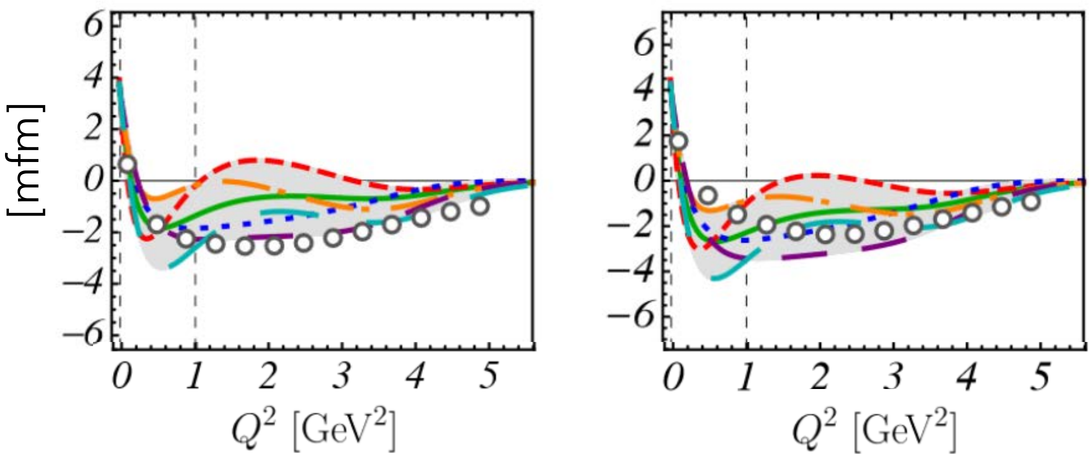

(W=1.38 GeV fixed)

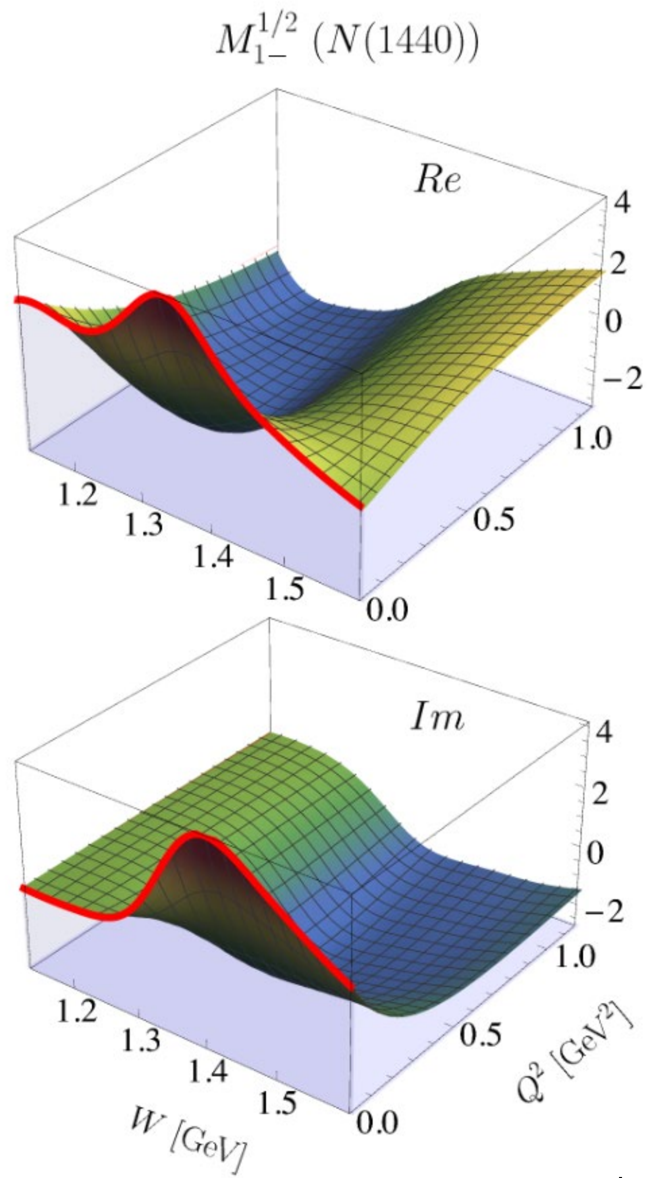

(Strategy 1 only)

- Zero-transition (agrees with MAID)
- Extensive exploration of parameter space reveals ambiguities in PWA and reflects systematic uncertainties
- Resonance parameters to be extracted

Summary

- Juelich-Bonn-Washington/JBW model: Phenomenology of excited baryons through coupled-channels, two- and three-body dynamics; data from Jlab, ELSA, MAMI, …
- Renewed effort to explore additional reaction channels in the last year:
  - $\gamma p \to K\Sigma$
  - $\pi N \to \omega N$
  - $\gamma^* p \to \pi N, \eta N$ (Electroproduction)
- Extensive exploration of parameter space leads to significant variance of some multipoles.
- Many "faint" resonance signals confirmed, others not
- Many hyperon polarization data changed (α_- decay parameter of Λ changed)

[D.G. Ireland et al., PRL, 1904.07616]

- How to find a minimal resonance spectrum? Model selection.

[J. Landay et al., PRD, 1810.00075]

- Data aspects: How to get solid statistical statements out of a heterogeneous data base dominated by systematic errors? [New experiments: Klong, Epecur,..]

(spare slides)

Outlook for electroproduction analysis

Reaction	Observable	Q^2 [GeV]	W [GeV]	Ref.
$ep \to e'p'\eta$	σ_U, σ_{LT}, σ_{TT}	$1.6 - 4.6$	$2.0 - 3.0$	[132]
	σ_U, σ_{LT}, σ_{TT}	$0.13 - 3.3$	$1.5 - 2.3$	[137]
	$d\sigma/d\Omega$	$0.25 - 1.5$	$1.5 - 1.86$	[138]
$ep \to e'K^+\Lambda$	P_N^0	$0.8 - 3.2$	$1.6 - 2.7$	[139]
	σ_U, σ_{LT}, σ_{TT}, $\sigma_{LT'}$	$1.4 - 3.9$	$1.6 - 2.6$	[140]
	P'_x, P'_z	$0.7 - 5.4$	$1.6 - 2.6$	[141]
	σ_T, σ_L, σ_{LT}, σ_{TT}	$0.5 - 2.8$	$1.6 - 2.4$	[142]
	P'_x, P'_z	$0.3 - 1.5$	$1.6 - 2.15$	[143]

Table 1: Overview of ηp and $K^+\Lambda$ electroproduction data measured at CLAS for different photon virtualities Q^2 and total energy W. Based on material provided by courtesy of D. Carman (JLab) and I. Strakovsky (GW).

- Many of these (and similar) data await analysis.
- Many more data to emerge at Jlab ($Q^2 = 5 - 12$ Gev^2)

e.g.: Carman, Joo, Mokeev, Few Body Syst. 61, 29 (2020)

- Approved Jlab experiments to study
  - Higher-lying nucleon resonances
  - Hybrid baryons
  - High-Q^2 transition between nonperturbative and perturbative QCD regimes

Klong will improve low-energy data situation

- The **only** low-energy differential cross section available:

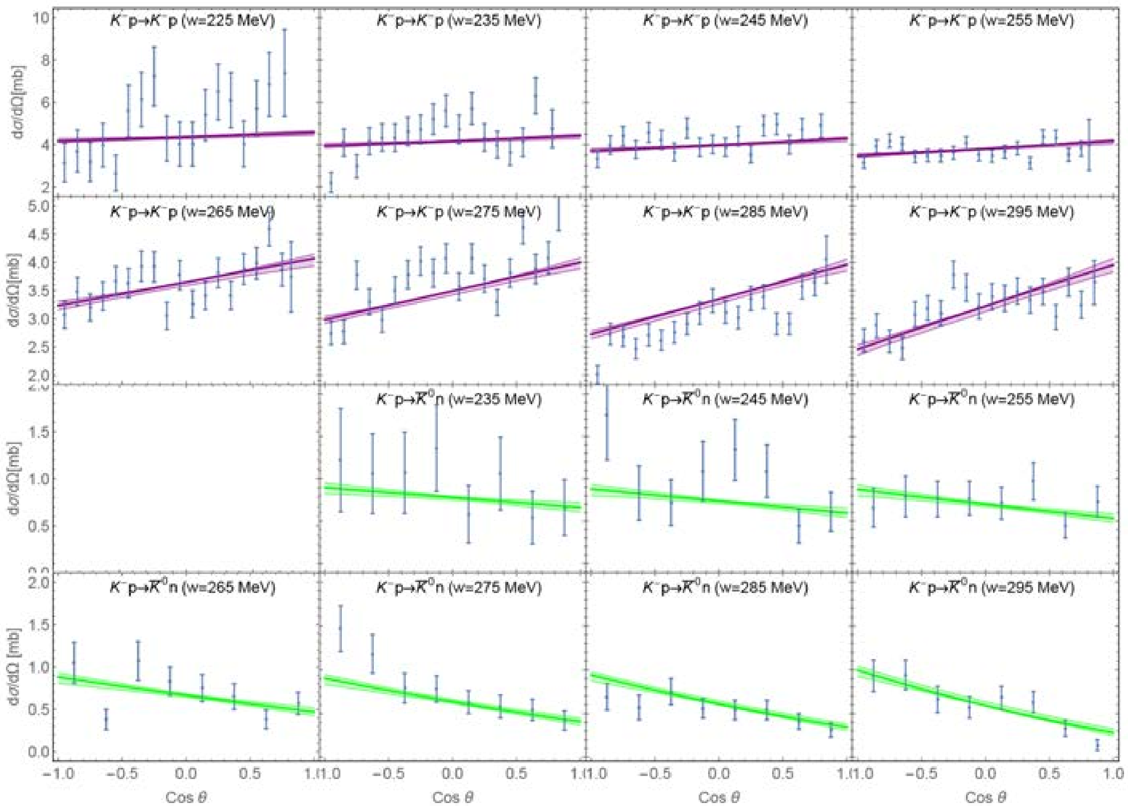

Data: [Mast 1976]
NLO: [Sadasivan 2018]

- P-wave important for NLO and NNLO chiral approaches
  → Not everything is S-wave… !

a_1: Three-particle propagation with helicities

- 2-body unitarity fixes only part of the interaction;

$$\tau^{-1}_{\lambda'\lambda}(\sigma_p) = \delta_{\lambda'\lambda}\tilde{K}^{-1}_n(s,\boldsymbol{p}) - \Sigma_{n,\lambda'\lambda}(s,\boldsymbol{p})\,,$$

$$\tilde{K}^{-1}_n(s,\boldsymbol{p}) = \sum_{i=0}^{n-1} a_i\sigma_p^i \quad \text{and} \quad \Sigma_{n,\lambda'\lambda}(s,\boldsymbol{p}) =$$

$$\int \frac{d^3k}{(2\pi)^3}\frac{\sigma_p^n}{(4E_k^2)^n}\frac{\hat{v}^*_{\lambda'}(P-p-k,k)\hat{v}_\lambda(P-p-k,k)}{2E_k(\sigma_p - 4E_k^2 + i\epsilon)}$$

n-times subtracted for convergence (n=2)

- The helicity of the ρ in flight can change!

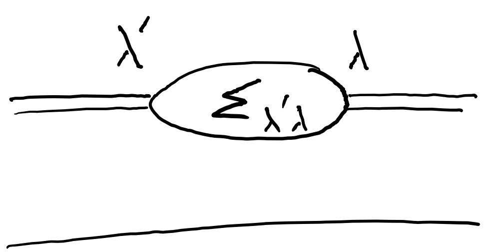

$\Big\}$ $\Sigma_{\lambda'\lambda} \neq 0$ for $\lambda' \neq \lambda$

a_1: 2-body input

- Global fit of 2-body sector across different isospins, including correlations across isospin [Mai 2019]

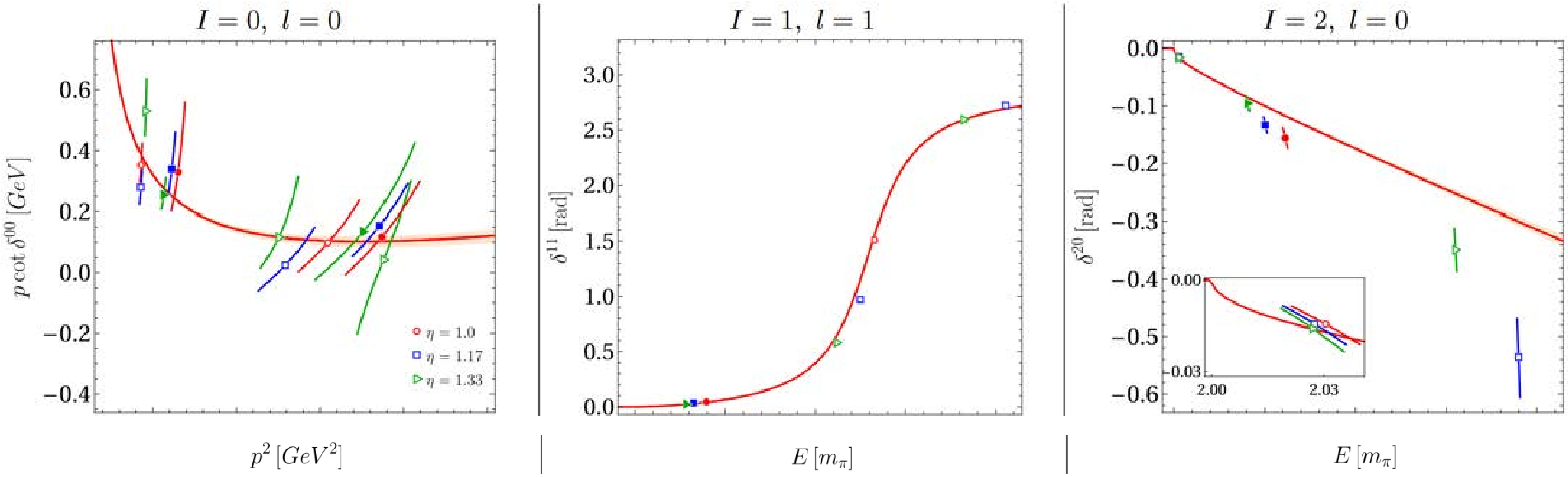

- Match to twice-subtracted dispersive expression to be used in three-body system

a_1: 4 different fits to 2 energy eigenvalues

- Fitted isobar-spectator interaction (case 1, 2) for $|\boldsymbol{p}| \leq 2\pi/L|(1,1,0)| \approx 2.69\ m_\pi$

$$C_{\ell'\ell}(s,\boldsymbol{p}',\boldsymbol{p}) = \sum_{i=-1}^{\infty} c^{(i)}_{\ell'\ell}(\boldsymbol{p}',\boldsymbol{p})(s-m_{a_1}^2)^i$$

- Case 2: a_1 is generated as pole even though no built-in singularity

Non-zero coefficients	No of fit parameters	x^2
c_{00}^0 (no built-in pole, m_{a1}=0)	1	9
c_{00}^0, c_{00}^1 (no built-in pole, m_{a1}=0)	2	0.15
g_0, g_2, m_{a1}	3	3.2
g_0, g_2, m_{a1}, c	4	10^{-7}

- Case 3, 4:

$$C_{\ell'\ell}(s,\boldsymbol{p}',\boldsymbol{p}) = g_{\ell'}\left(\frac{|\boldsymbol{p}'|}{m_\pi}\right)^{\ell'}\frac{m_\pi^2}{s-m_{a_1}^2}g_\ell\left(\frac{|\boldsymbol{p}|}{m_\pi}\right)^{\ell} + c\,\delta_{\ell'0}\delta_{\ell 0}$$

- In these cases, there is a built-in singularity, leading to resonance poles

a_1: Properties of 4-parameter fit

- 4 parameters for 2 energy eigenvalues produce remarkably stable results with resonance poles in a well-defined region and not all over the place.
- The D-wave coupling and a_1-mass are strongly correlated
  - Makes sense because D-wave a_1 self energy is mostly real

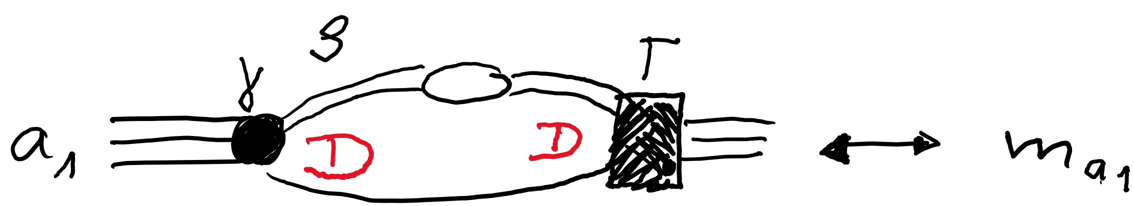

$$T^{Pole} = \frac{\Gamma\,\Gamma^\dagger}{s - m_{a_1}^2 - \Sigma_S - \Sigma_D}$$

$\Gamma =$ 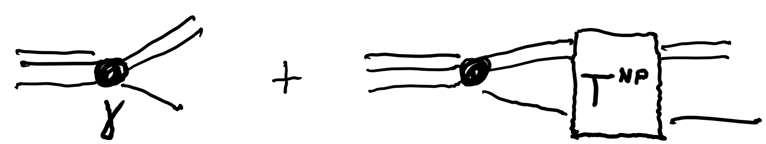

"Two-potential formalism"

a_1: Results – overview (4 parms)

Cluster: Large c and g_s compensate; disappears with c=0

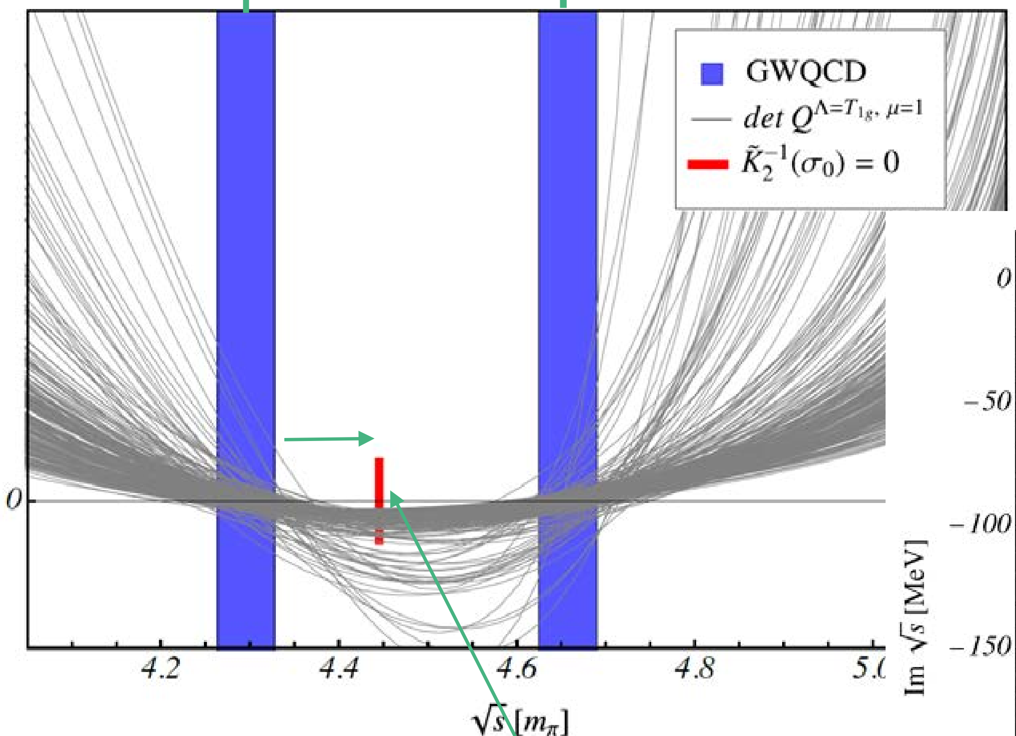

$$0 = \det\left[B(s) + C(s) - E_L\left(\tilde{K}_2^{-1}(s) - \Sigma_2^L(s)\right)\right]_{(\lambda'\lambda)(p'p)}$$

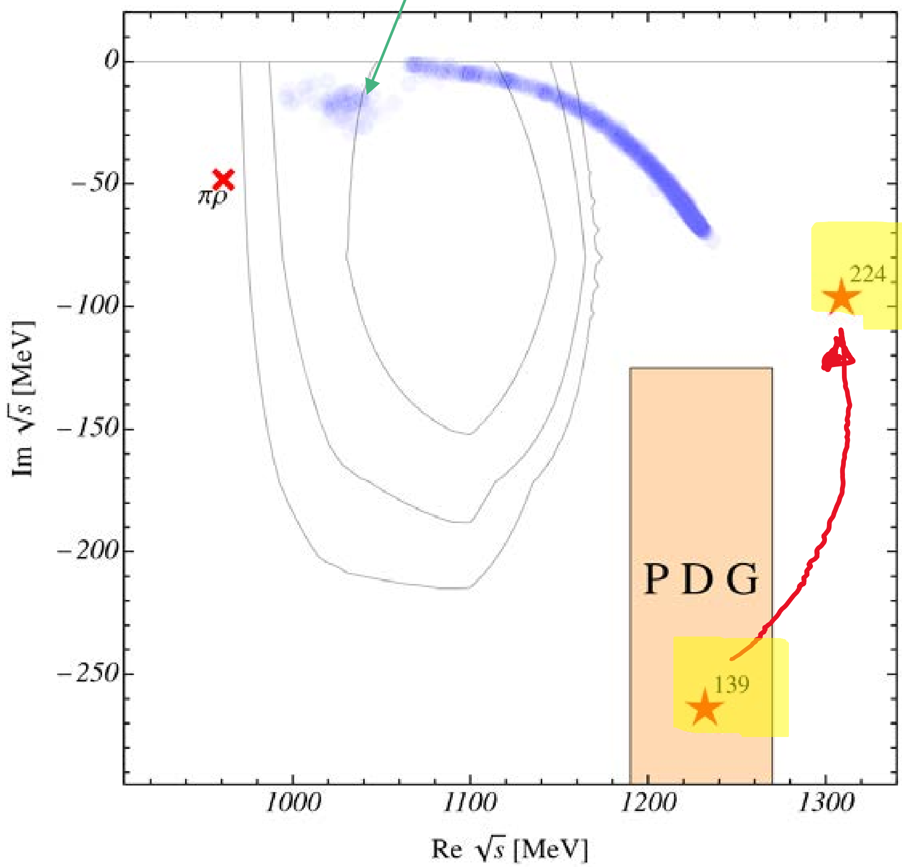

a_1: Branching ratios

- Calculate the residue at the pole:

$$\mathrm{Res}(T^{c}_{\ell'\ell}(\sqrt{s})) = \tilde{g}_{\ell'}\tilde{g}_{\ell}$$

- This result is not as reliable as pole position/existence of a_1
- More energy eigenvalues needed to better pin down the decay channels
- Other isospins needed, e.g., $(\pi\sigma)_P$ [Molina 2021]

"**Branching ratios**" in 3B decays are momentum –dependent, complex pole residues

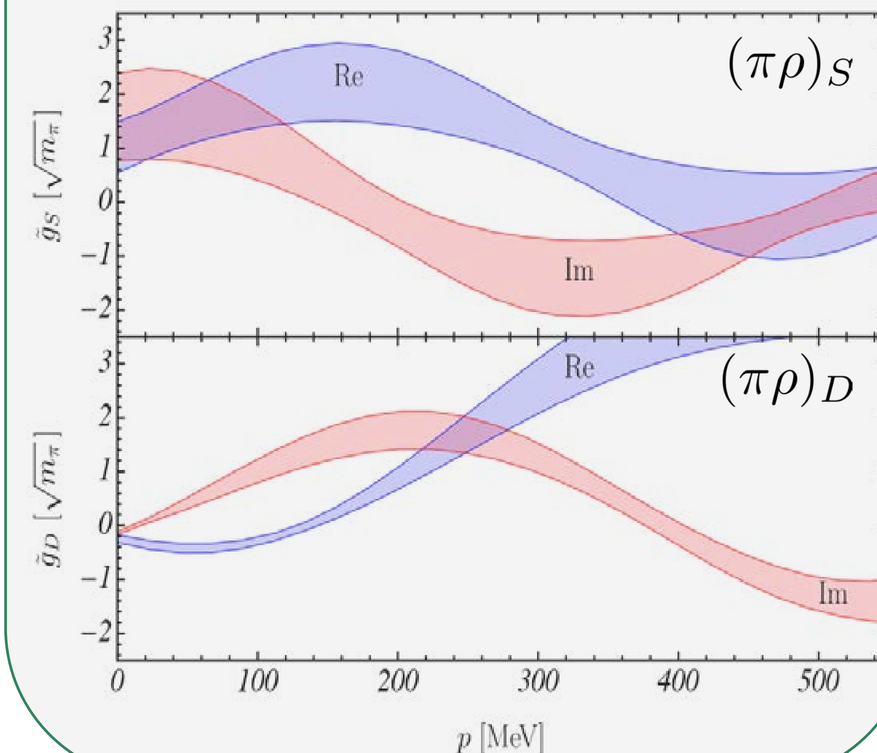

PDG Changes

- Changes from one PDG edition to another
- New states in red
- Upgrade existing states
- Removal older & lower rated states
- All changes come from Partial-wave analysis (PWA) of photon-induced reactions.

Table from [Crede]

Table 9. (Colour online) Baryon Summary Table for N^* and Δ resonances includin
recent changes from PDG 2010 [2] to PDG 2012 [1].

N^*	$J^P\ (L_{2I,2J})$	2010	2012	Δ	$J^P\ (L_{2I,2J})$	2010	2012
p	$1/2^+\ (P_{11})$	****	****	$\Delta(1232)$	$3/2^+\ (P_{33})$	****	****
n	$1/2^+\ (P_{11})$	****	****	$\Delta(1600)$	$3/2^+\ (P_{33})$	***	***
$N(1440)$	$1/2^+\ (P_{11})$	****	****	$\Delta(1620)$	$1/2^-\ (S_{31})$	****	****
$N(1520)$	$3/2^-\ (D_{13})$	****	****	$\Delta(1700)$	$3/2^-\ (D_{33})$	****	****
$N(1535)$	$1/2^-\ (S_{11})$	****	****	$\Delta(1750)$	$1/2^+\ (P_{31})$	*	*
$N(1650)$	$1/2^-\ (S_{11})$	****	****	$\Delta(1900)$	$1/2^-\ (S_{31})$	**	**
$N(1675)$	$5/2^-\ (D_{15})$	****	****	$\Delta(1905)$	$5/2^+\ (F_{35})$	****	****
$N(1680)$	$5/2^+\ (F_{15})$	****	****	$\Delta(1910)$	$1/2^+\ (P_{31})$	****	****
$N(1685)$			*				
$N(1700)$	$3/2^-\ (D_{13})$	***	***	$\Delta(1920)$	$3/2^+\ (P_{33})$	***	***
$N(1710)$	$1/2^+\ (P_{11})$	***	***	$\Delta(1930)$	$5/2^-\ (D_{35})$	***	***
$N(1720)$	$3/2^+\ (P_{13})$	****	****	$\Delta(1940)$	$3/2^-\ (D_{33})$	*	**
$N(1860)$	$5/2^+$		**				
$N(1875)$	$3/2^-$		***				
$N(1880)$	$1/2^+$		**				
$N(1895)$	$1/2^-$		**				
$N(1900)$	$3/2^+\ (P_{13})$	**	***	$\Delta(1950)$	$7/2^+\ (F_{37})$	****	****
$N(1990)$	$7/2^+\ (F_{17})$	**	**	$\Delta(2000)$	$5/2^+\ (F_{35})$	**	**
$N(2000)$	$5/2^+\ (F_{15})$	**	**	$\Delta(2150)$	$1/2^-\ (S_{31})$	*	*
~~$N(2080)$~~	D_{13}	**		$\Delta(2200)$	$7/2^-\ (G_{37})$	*	*
~~$N(2090)$~~	S_{11}	*		$\Delta(2300)$	$9/2^+\ (H_{39})$	**	**
$N(2040)$	$3/2^+$		*				
$N(2060)$	$5/2^-$		**				
$N(2100)$	$1/2^+\ (P_{11})$	*	*	$\Delta(2350)$	$5/2^-\ (D_{35})$	*	*
$N(2120)$	$3/2^-$		**				
$N(2190)$	$7/2^-\ (G_{17})$	****	****	$\Delta(2390)$	$7/2^+\ (F_{37})$	*	*
~~$N(2200)$~~	D_{15}	**		$\Delta(2400)$	$9/2^-\ (G_{39})$	**	**
$N(2220)$	$9/2^+\ (H_{19})$	****	****	$\Delta(2420)$	$11/2^+\ (H_{3,11})$	****	****
$N(2250)$	$9/2^-\ (G_{19})$	****	****	$\Delta(2750)$	$13/2^-\ (I_{3,13})$	**	**
$N(2600)$	$11/2^-\ (I_{1,11})$	***	***	$\Delta(2950)$	$15/2^+\ (K_{3,15})$	**	**
$N(2700)$	$13/2^+\ (K_{1,13})$	**	**				

Pion Electroproduction – data base

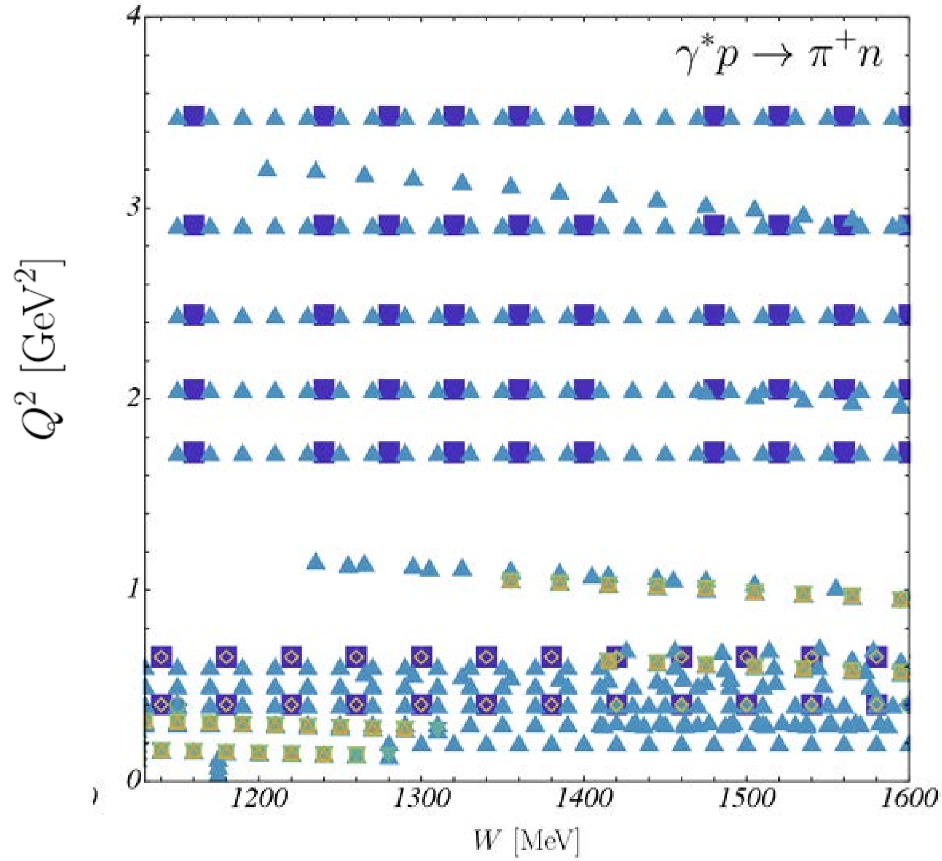

Type	N_{data}
ρ_{LT}	–
$\rho_{LT'}$	4354
σ_L	2
$d\sigma/d\Omega$	32813
$\sigma_T + \epsilon\sigma_L$	144
σ_T	2
σ_{LT}	106
$\sigma_{LT'}$	192
σ_{TT}	91
K_{D1}	–
P_Y	–

- Data base grown over decades with recent input mostly by CLAS, MAMI.
- Far from complete: Kinematic gaps & consistency issues. Need to combine information from different (W, Q^2) regions
- Need to combine information from simultaneous analysis of different final states ($\pi N/\eta N/KY/\pi\pi N,\ldots.$) to extract resonance helicity couplings

Pion Electroproduction – data base

Extended Q^2 up to 6 GeV^2 to check dependence of results

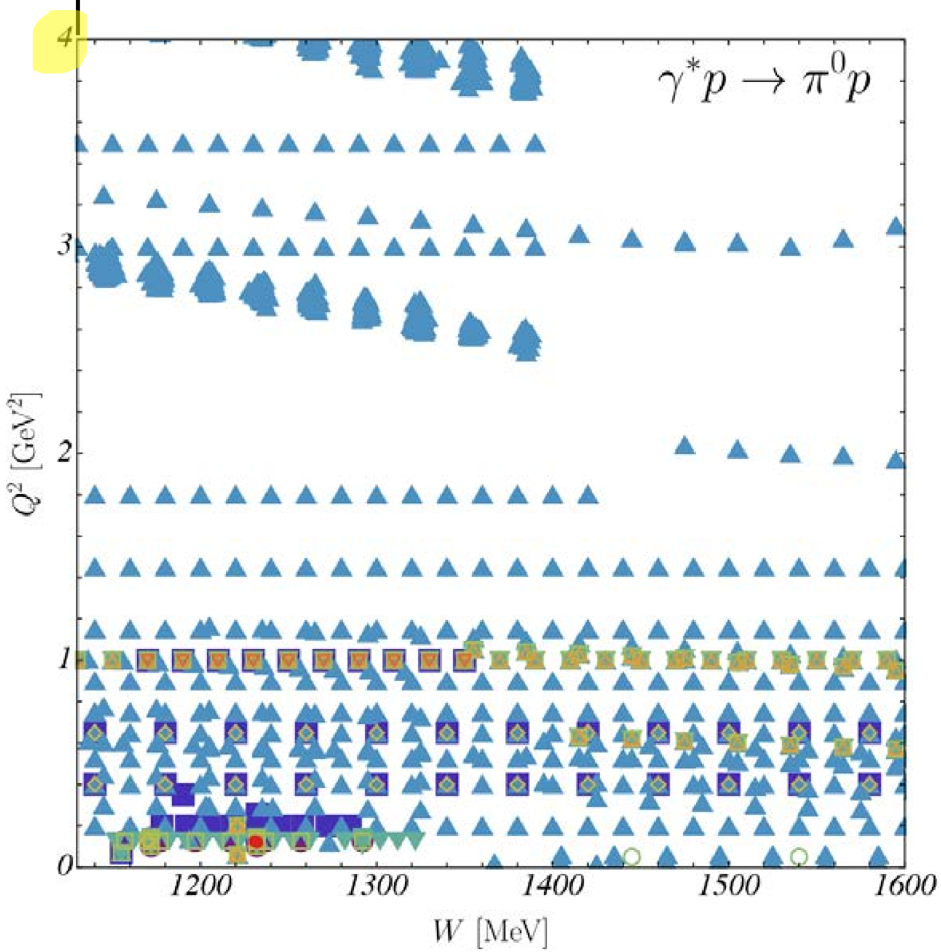

Type	N_{data}
● ρ_{LT}	45
■ $\rho_{LT'}$	2644
◆ σ_L	–
▲ $d\sigma/d\Omega$	39942
▼ $\sigma_T + \epsilon\sigma_L$	318
○ σ_T	10
□ σ_{LT}	312
◇ $\sigma_{LT'}$	198
△ σ_{TT}	266
▽ K_{D1}	1527
● P_Y	2

Structure functions

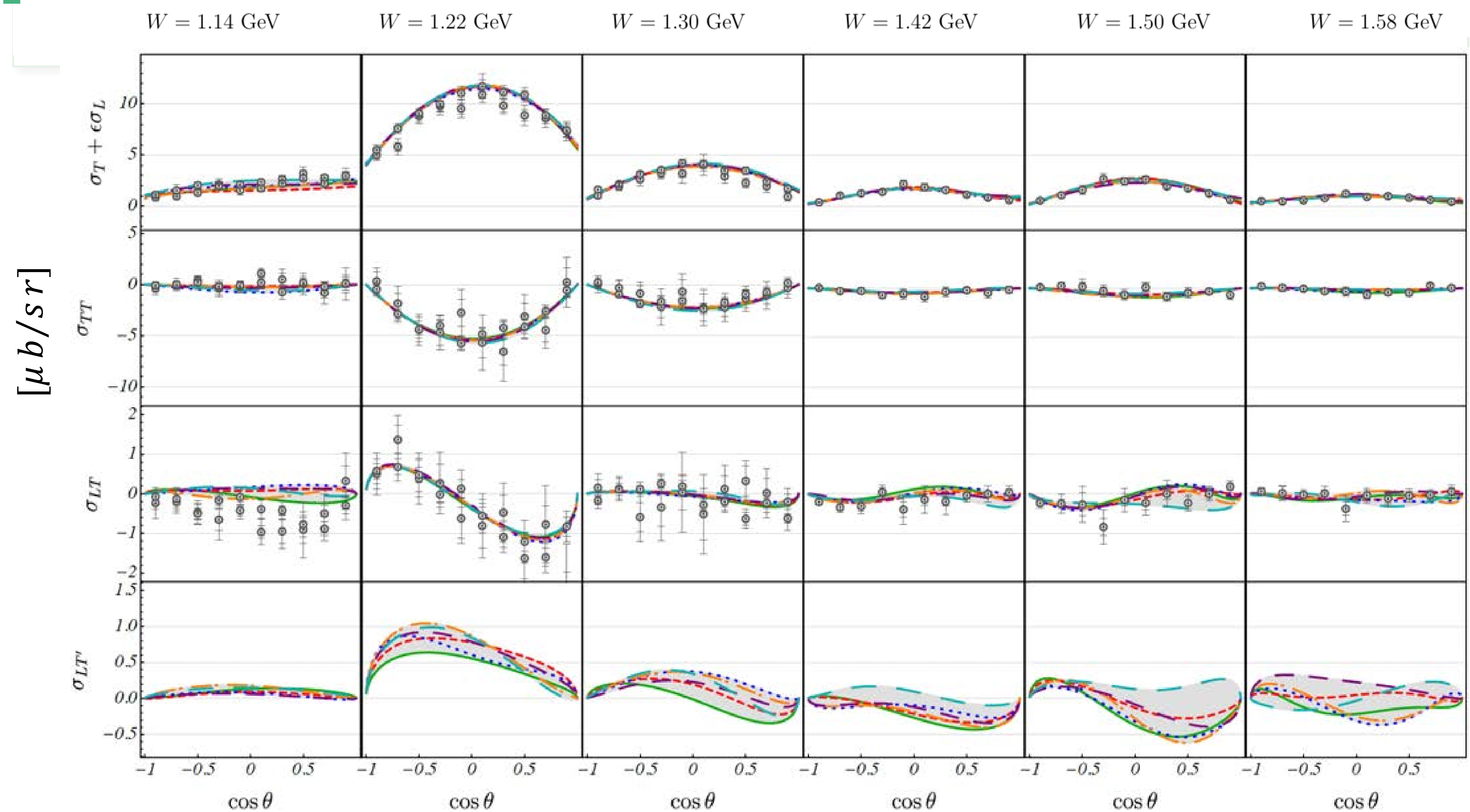

$Q^2 = 0.9$ Gev^2, $\pi^0 p$

data: CLAS, Phys. Rev. C (2003) 0301012 [nucl-ex], Phys. Rev. Lett. (2002) 0110007 [hep-ex]

η Electroproduction

[M. Mai et al., arXiv: 2111.04774]

- $N^{\eta p}_{data} = 1,874$ (only $d\sigma/d\Omega$) (84,842 in total)
- kinematic range: $0 < Q^2 < 4$ GeV^2, $1.13 < W < 1.6$ GeV
- 8 different fit strategies: 4 with standard χ^2, 4 with weighted χ^2 to account for the smaller $N^{\eta p}_{data}$ $\rightarrow$ better data description with weighted fit strategies:

Selected fit results: $\gamma^* p \rightarrow \eta p$ at $W = 1.5$ GeV, $Q^2 = 1.2$ GeV^2. Data: Denizli et al. (CLAS) PRC 76 (2007)

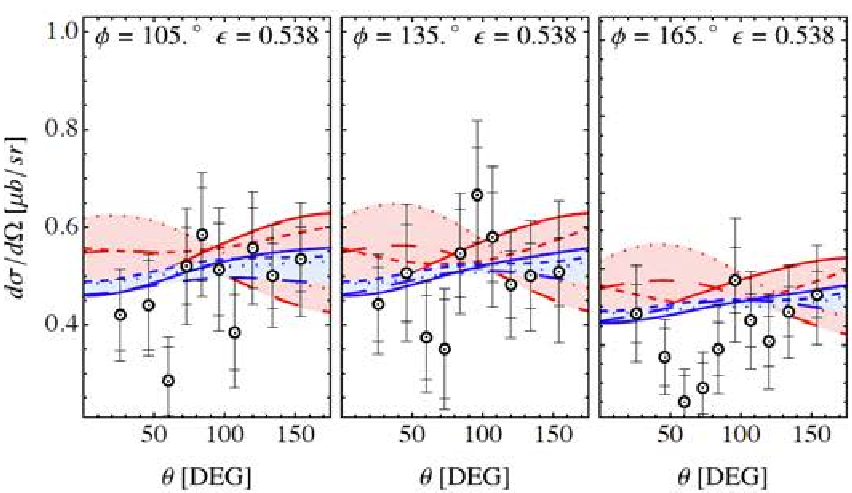

Selected multipoles at $W = 1535$ MeV

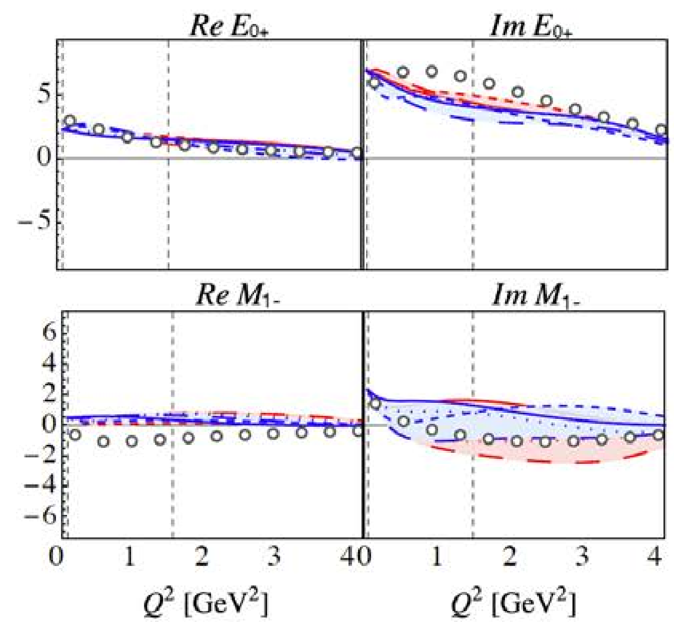

Dots: eta-MAID, arXiv:0110034

Extraction of resonance helicity couplings at the pole is under way

Channel space

- Jülich-Bonn-Washington approach has the same channel space as ANL/Osaka (former EBAC) approach

μ	$J^P =$	$\frac{1}{2}^-$	$\frac{1}{2}^+$	$\frac{3}{2}^+$	$\frac{3}{2}^-$	$\frac{5}{2}^-$	$\frac{5}{2}^+$	$\frac{7}{2}^+$	$\frac{7}{2}^-$	$\frac{9}{2}^-$	$\frac{9}{2}^+$
1	πN	S_{11}	P_{11}	P_{13}	D_{13}	D_{15}	F_{15}	F_{17}	G_{17}	G_{19}	H_{19}
2	$\rho N(S=1/2)$	S_{11}	P_{11}	P_{13}	D_{13}	D_{15}	F_{15}	F_{17}	G_{17}	G_{19}	H_{19}
3	$\rho N(S=3/2, \|J-L\|=1/2)$	—	P_{11}	P_{13}	D_{13}	D_{15}	F_{15}	F_{17}	G_{17}	G_{19}	H_{19}
4	$\rho N(S=3/2, \|J-L\|=3/2)$	D_{11}	—	F_{13}	S_{13}	G_{15}	P_{15}	H_{17}	D_{17}	I_{19}	F_{19}
5	ηN	S_{11}	P_{11}	P_{13}	D_{13}	D_{15}	F_{15}	F_{17}	G_{17}	G_{19}	H_{19}
6	$\pi\Delta(\|J-L\|=1/2)$	—	P_{11}	P_{13}	D_{13}	D_{15}	F_{15}	F_{17}	G_{17}	G_{19}	H_{19}
7	$\pi\Delta(\|J-L\|=3/2)$	D_{11}	—	F_{13}	S_{13}	G_{15}	P_{15}	H_{17}	D_{17}	I_{19}	F_{19}
8	σN	P_{11}	S_{11}	D_{13}	P_{13}	F_{15}	D_{15}	G_{17}	F_{17}	H_{19}	G_{19}
9	$K\Lambda$	S_{11}	P_{11}	P_{13}	D_{13}	D_{15}	F_{15}	F_{17}	G_{17}	G_{19}	H_{19}
10	$K\Sigma$	S_{11}	P_{11}	P_{13}	D_{13}	D_{15}	F_{15}	F_{17}	G_{17}	G_{19}	H_{19}

S-, t- and u-channel exchanges

- 21 s-channel states (resonances) coupling to πN, ηN, $K\Lambda$, $K\Sigma$, $\pi\Delta$, ρN.
- t- and u-channel exchanges ("*background*"):

	πN	ρN	ηN	πΔ	σN	KΛ	KΣ
πN	N,Δ,$(\pi\pi)_\sigma$, $(\pi\pi)_\rho$	N, Δ, Ct., π, ω, a_1	N, a_0	N, Δ, ρ	N, π	Σ, Σ*, K*	Λ, Σ, Σ*, K*
ρN		N, Δ, Ct., ρ	-	N, π	-	-	-
ηN			N, f_0	-	-	K*, Λ	Σ, Σ*, K*
πΔ				N, Δ, ρ	π	-	-
σN					N, σ	-	-
KΛ						Ξ, Ξ*, f_0, ω, ϕ	Ξ, Ξ*, ρ
KΣ							Ξ, Ξ*, f_0, ω, ϕ, ρ

Is there a system behind this?

2→ 3 and 3→3 body unitarity

- See last part of this lecture: Unitarity requires certain transition amplitudes

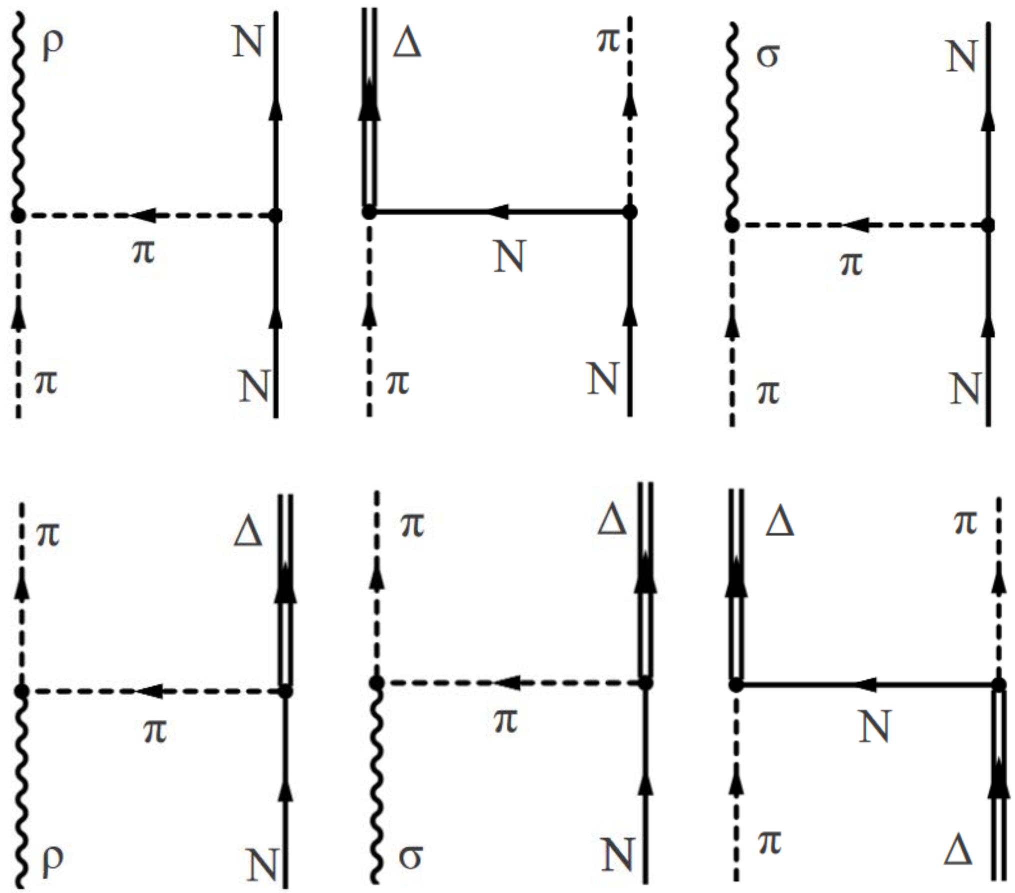

2→3

3→3